Bidecadal Thermal Changes in the Abyssal Ocean

Carl Wunsch

Department of Earth and Planetary Sciences

Harvard University

Cambridge MA 02138

email: cwunsch@fas.harvard.edu

Patrick Heimbach

Department of Earth, Atmospheric and Planetary Sciences

Massachusetts Institute of Technology

Cambridge MA 02139

December 28, 2013

Abstract

A dynamically consistent state estimate is used for the period 1992-2011 to describe the changes in oceanic temperatures and heat content, with an emphasis on determining the noise background in the abyssal (below 2000 m) depths. Interpretation requires close attention to the long memory of the deep ocean, and implying that meteorological forcing of decades to thousands of years ago should still be producing trend-like changes in abyssal heat content. At the present time, warming is seen in the deep western Atlantic and Southern Ocean, roughly consistent with those regions of the ocean expected to display the earliest responses to surface disturbances. Parts of the deeper ocean, below 3600 m, show cooling. Most of the variation in the abyssal Pacific Ocean is comparatively featureless, consistent

with the slow, diffusive, approach to a steady state expected there. In the global average, changes in heat content below 2000 m are roughly 10% of those inferred for the upper ocean over the 20 year-period. A useful global observing strategy for detecting future change has to be designed to account for the different time and spatial scales manifested in the observed changes. If the precision estimates of heat content change are independent of systematic errors, determining oceanic heat uptake values equivalent to 0.1 W/m^2 is possibly attainable over bidecadal periods.

1 Introduction

The major observational obstacle to understanding the role of the ocean in climate is the extreme brevity of the instrumental record in a system having some memory exceeding several thousands of years. Data sets depicting the global interior ocean state begin with high accuracy altimetry only in 1992. The Argo array became quasi-global in the mid-2000s. Assuming that these technologies continue to be supported (by no means clear), the community will ultimately have comparatively long records at least of the phenomena visible in upper-ocean hydrographic profiles and sea surface elevation.

Even in this recent period, major spatial and temporal inhomogeneities exist in these and related data. The main purpose of this paper is to examine the nature of the thermal variability in the deep ocean (below about 2000 m). At the present time, the Argo array (Roemmich et al., 2009), supplemented by elephant seal data (Roquet et al., 2013), is confined to the upper 2000 m and with the bulk of the extant values above 1000 m. Altimetric data respond to motions over the entire water column, although the partitioning of the motions they represent remains the subject of considerable debate. Most of the available abyssal measurements are sparse deep CTD profiles (Fig. 1) from hydrographic programs, sometimes designed to depict special regions (e.g., the Kuroshio or the Nordic Seas).

Figure 1 here

An important wider issue is the nature of a practical set of future observations capable of providing a basis for understanding of ongoing ocean changes. At the end, some comments will be made about this problem, drawing on the results of the present analysis.

Much of the recent literature focuses on the ability to detect past and ongoing trends in ocean temperatures and heat content. The reality and magnitude of such changes is *not* the goal here; rather it is to characterize the extent to which more general variability can be detected using the much more dense observational system of the last 10-20 years. On the other hand, some order of magnitude numerical values are helpful for context.

Consider, for example, that greenhouse gas warming of the ocean is widely believed to be of order 1 W/m^2 (e.g., Hansen et al., 2005) or less. The volume of the ocean is about 1.3×10^{18} m^3. Using a mean density of 1038 kg/m^3, the total mass is about 1.34×10^{21} kg, and with a heat capacity of roughly 3.8×10^3 J/kg/°C, the global heat capacity is approximately 5.4×10^{24} J/°C. A heating rate of 1 W/m^2, if maintained for 20 years, produces an energy content change of about 2.2×10^{23} J for a change in global ocean mean temperature of about 0.04°C. If the heating were confined to the upper 700 m, then based on a mean ocean depth of about 3700 m, the temperature change is increased to about 0.2°C, and if all confined to the region below that depth, would be about 0.05°C (see Table 1). Recent observationally-based estimates (Church et al., 2011) produce estimates closer to 0.5 W/m^2, exacerbating the detection problem. (That the atmospheric radiation budget, includes such poorly determined elements as changes in aerosals and cloud distributions is a major impetus to determining actual ocean heat storage changes.) Alternatively, a 1 mm/year thermally-induced change in global mean sea level, if sustained for 20 years, is consistent with a full ocean volume mean temperature change of about 0.03°C, although important spatial variations exist in the sea level response to a fixed temperature change.

Table 1 here

An important question, pursued elsewhere, is whether available observations alone are capable of determining mean ocean temperatures, and the related heat content changes with time, to accuracies and precisions useful at these levels? Estimating the global average change is especially challenging and is here only a by-product.

Historically, deep hydrographic measurements (below a few hundreds or perhaps 1000 m) have been both difficult and expensive to acquire (see Abraham et al., 2013). The consequence has been sampling by a few, rare (in a multi-decadal or centennial context), fragmentary top-to-bottom hydrographic stations and sections. Systematic global surveys did not begin until the era of the World Ocean Circulation Experiment, circa 1990. Fig. 1 displays all of the oceanic temperature data (all CTD values) below 2000 m and below 3600 m since 1992 and used here (taken from the World Ocean Data Base 2009 of NOAA). Elephant seal temperature data do exist below 2000 m, but are rare and are not included. By some standards (e.g., paleoceanography; see Huybers and Wunsch, 2010), an impressive amount of data does exist: an evaluation of their adequacy can only be made in the context of the signal-to-noise structure and magnitudes at depth. Determining time changes with these data sets involves segregating them by interval with a consequent great reduction in the numbers available in any year or multiple of a year. To convey some of the observational difficulties, Fig. 2 displays the space-time standard deviation as a function of depth (not area-weighted) as well as the standard deviation of the annual cycle. Accurate removal of the annual cycle and the temporal mean from individual data points is a major problem in the upper ocean, but not discussed here.

Figure 2 here

As a consequence, many papers have been published that simply assume no significant changes take place in the deep ocean over the historical period. Shifts in the deep ocean properties may indeed be so slight that their neglect in discussions of heat uptake and sea level change is justified. The history of exploration suggests, however, that blank places on the map have either been assumed to be without any interesting features and dropped from further discussion, or at the other extreme, filled with "dragons" invoked to explain strange reports.[1] It is also physically possible that in a search for abyssal trends, that the higher frequency, higher wavenumber, noise is negligible compared to the signals. In that view, the existing reports of deep trends based upon hydrographic lines (Roemmich and Wunsch, 1984; Bryden et al., 1996; Joyce et al., 1999; Purkey and Johnson, 2010; and others) are adequate. Recently, Balamaseda et al., (2013) offered estimates of abyssal changes with claimed accuracies of order of 0.01 W/m^2 (0.0004°C temperature change equivalent over 20 years) below 700 m. If that accuracy has indeed been obtained, the sparse coverage, perhaps extended to the scope of the WOCE hydrographic survey, repeated every few decades, is sufficient.

Given the combination of the high societal stakes in the accurate estimation of global heating rates and sea level rise, and the fundamental science questions of understanding of oceanic variability, direct confirmation or refutation of this sufficiency hypothesis is essential. If it proves false, discussion can take place concerning the design of an adequate system. One purpose of this paper is to make a start towards answering the question of adequacy.

2 A Framework: The State Estimate

Apart from the large-scale hydrographic survey done as part of WOCE (see Talley, 2007), most direct ocean measurements have been made at the sea surface (altimetry, sea surface temperature, drifters), or obtained from XBTs (some reaching to order 750 m), and more recently

[1] A nice example can be seen in G. de Jode (1593) *Speculum Orbis Terrarum*, Antwerp.

from Argo floats, profiling primarily to 1000 m, and more recently, many now to 2000 m (e.g., von Schuckmann and Le Traon, 2011; an extended listing of the available data sets is in Table 1 of Wunsch and Heimbach, 2013a). Hypothetically, a highly accurate estimate of e.g., heat and salt content changes in the upper ocean, coupled with altimetric, meteorological etc., measurements would allow inference of the deep ocean changes as residuals in the data from subtraction of upper ocean contributions. The strategy used here is to exploit both this idea, and the deep data that do exist, through the vehicle of a constrained general circulation model. How well the upper ocean is determined, and thus the accuracy of the abyssal residuals so calculated, is still not so clear.

The ECCO[2] "state estimate" has been described in a number of places (e.g., Wunsch and Heimbach, 2007, 2013a,b). In summary, it is a weighted least-squares fit of a general circulation model (an evolved version of the MITgcm; see Marshall et al., 1997, and Adcroft et al., 2004, for early forms) to the quasi-global data sets (which include the atmospheric forcing) using Lagrange multipliers. The estimate has 1^o zonal resolution and a meridional resolution ranging from about 0.25^o near the equator and poles to 1^o at mid-latitudes. An initial (then-adjusted) meteorological forcing is derived from the ECMWF ERA-Interim reanalysis (Dee et al., 2011). A numerical algorithm for fitting using the Lagrange multipliers is sometimes known as the "adjoint method" or in meteorology as "4DVAR." The specific estimate used is labelled version 4, revision 5, and in contrast to earlier estimates includes a full sea ice model (Losch et al., 2010; Fenty and Heimbach, 2013), and extends to the North Pole (see Forget et al., 2013, in preparation, for full details).[3]

[2]Estimating the Circulation and Climate of the Oceans; here using the MIT-AER version

[3]The final state estimate is obtained from the free running forward model, using the adjusted control parameters. In this particular case, the inference of a calibration discrepancy between the infrared estimate of sea surface temperature, and that of the Advanced Microwave Scanning Radiometer, whose data became available in 2002,

Very recently, Abraham et al. (2013) have published a useful discussion of the methods used both historically and today for direct ocean temperature measurements including, especially, the ongoing debates about systematic errors in the different data sets. The present state estimate uses all of the post-1991 data types they discuss, but combines them also with the continuous high density altimetric height and other measurements, as well as with the best-initial-estimate we could obtain of the air-sea heat transfers. Thus the direct thermal measurements are combined with numerically much more numerous estimates of atmospheric heat transfers, implied sea level shifts and other data.

Note that over the great volume of the oceans, the ECCO-state is in slowly time-evolving geostrophic, hydrostatic balance that, unlike most "data assimilation" products, satisfies the model equations without any artificial sources or sinks or forces. The state estimate is from the free running, but adjusted, model and hence satisfies all of the governing model equations, including those for basic conservation of mass, heat, momentum, vorticity, etc. up to numerical accuracy.

Data assimilation schemes running over decades are usually labelled "reanalyses." Unfortunately, these cannot be used for heat or other budgeting purposes because of their violation of the fundamental conservation laws; see Wunsch and Heimbach (2013a) for discussion of this important point. The problem necessitates close examination of claimed abyssal warming accuracies of 0.01 W/m^2 based on such methods (e.g., Balmaseda et al., 2013).

As with other extant estimates, the present state estimate does not yet account for the geothermal flux at the sea floor whose mean values (Pollack et al., 1993) are of order 0.1 W/m^2, and which are minute relative to the surface heating. But they are not negligible compared either

led to a small ad hoc adjustment of the imposed surface air-temperature field in the final calculation. Both products are discussed by Reynolds et al. (2007); see also Chelton and Wentz (2005).

to the vertical heat transfer into the abyss from above (measured e.g., by $\kappa\,\partial T/\partial z$, where κ is a vertical diffusion coefficient; cf. Emile-Geay and Madec, 2009)[4] or the change in atmospheric radiative forcing. Absence of this abyssal heating is one of the reasons we do not emphasize what prove to be weak trends in the state estimate.

The methodology used by Kouketsu et al. (2011) is analogous to that employed here, although some of their inferences are different. Those differences and their possible causes are discussed later.

A total change in heat content, top-to-bottom, is found (discussed below) of approximately 4×10^{22} J in 19 years, for a net heating of 0.2±0.1 W/m^2, smaller than some published values (e.g., Hansen et al., 2005, 0.86±0.12 W/m^2; Lyman et al., 2010, 0.63±0.28 W/m^2; or von Schuckmann and Le Traon, 2011, 0.55±0.1 W/m^2; but note the differing averaging periods), but indistinguishable from the summary Fig. 14 of Abraham et al. (2013). Perhaps coincidentally, it is similar to the 135-year 700 m depth ocean rate of 0.2±0.1 W/m^2 of Roemmich et al. (2012). On multi-year time-scales accessible with a 20-year record, the present estimate is sensitive in the upper ocean to the prior estimates of atmospheric heat transfers. In contrast, the abyssal ocean response to multi-year surface thermodynamic variability is expected to be confined to small convective regions, boundary regions of baroclinic deformation radius width, and near the equator.

Figure 3 here

Fig. 3 displays the temperature and salinity census in logarithmic units at the start of the state estimate. The ocean is dominated by the very cold, intermediate salinity values of the vast abyssal interior and a calculation of net heat content change requires measurements of this

[4] A vertical temperature gradient of 1°C/1000 m and a (low) eddy diffusion coefficient of 10^{-5} m^2/s, produces a diffusive heat transport of about 0.04 W/m^2.

cold-water sphere with volume averages precisions consistent with Table 1.

Misfits

The most basic test of any least-squares state estimate is the extent to which the diverse data sets have been fit to the model trajectory. A full discussion of the misfits to the approximately 2×10^9 data constraints in the estimate requires far more space than is available here. As a representative of the complete discussion, the misfits between the CTD and the state estimate in different depth ranges are shown in Figs. 4, 5. Apart from the outliers expected in the χ_2^2 distribution characterizing least-squares residuals, almost all values are close to zero and obvious large-scale systematic offsets do not appear. Regional misfits do remain, but are generally confined to comparatively small ocean volumes. The great bulk of the state estimate is in geostrophic, hydrostatic balance and which tends to control the transport properties of the poorly resolved boundary currents and other special regions.

Figure 4 here

Figure 5 here

More generally, the solution, in terms of misfits to *all* of the data (whose numbers are dominated by the meteorological values and altimetry), is deemed adequate for analysis. No claim is made that the results are "right", only that they represent one well-defined estimate in terms of specific physics and data and allocated errors.

2.1 Timescales

One of the fundamental characteristics of the ocean as it influences climate on decadal and longer time-scales is its long memory—the main reason why the brevity of the instrumental record is so frustrating. Simple calculations show that the ocean responds, and thus remembers, on time scales of seconds out to thousands of years. When interpreting measurements of changes, any assumption that they have been generated by disturbances from the recent past has to be examined and justified. The question arises specifically in the determination of the initial conditions in a calculation of change. Note that the control vector of the state estimate explicitly contains the system initial conditions—hydrography and flow.

A large number of physical mechanisms operates in the ocean as it responds dynamically and kinematically to external disturbances. Many of these adjustments will occur on time scales that are brief compared to a two-decadal time-span, including Kelvin-like coastal and low-latitude Rossby waves, advective adjustments such as Ekman pumping changes, convective responses to changing ice-cover, and changes in eddy bolus transports. Spatial scales will range from deformation radii motions and property shifts to those extending to entire ocean basins—depending directly on the physical mechanisms. On the other hand, many such processes will be present with time scales extending from multiple decades out to thousands of years. From the point of view of basin-scale heat content changes measured on a bidecadal time-scale, responses are also expected to the initial conditions in 1992. These reflect any disequilibrium between modern meteorological forcing and the memory embedded in the deep ocean of fluctuations arising from long-ago disturbances.

Using the dual (adjoint) model of the MITgcm used to obtain the state estimates, Heimbach et al. (2011) showed that changes in North Atlantic Ocean meridional heat transport exhibited a noticeable response to advected temperature changes from preceding decades and extending to great distances globally. The many mechanisms known to operate in oceanic temporal adjustment are present in the model and state estimate, and they depend strongly upon region. In contrast, in another calculation employing the state estimate, Wunsch and Heimbach (2008) calculated the time for a passive tracer to reach equilibrium values over ocean basin scales, an example of which is reproduced in Fig. 6, with time-scales depending upon the region, ranging from order 100 years to nearly 10,000 years (in the abyssal North Pacific Ocean). These long time-scales are easily rationalized in a number of ways, including the diffusion times required to ultimately erase spatial gradients. For example, the diffusion $e-$folding times are of order L^2/K where L is a characteristic length, and K is a diagonal element of the diffusion tensor. If $L \approx 10^4$ km (width of the Pacific Ocean) and a horizontal diffusion coefficient is in the range of 500-1000 m^2/s (e.g., Ferreira et al., 2005) the characteristic time is of order 3000y. Vertical-distances and diffusion will produce similar times. Additional long time scales can be derived e.g., from ocean volumes and their advective renewal times.

Figure 6 here

Depending upon geographical region, depth range, and spatial scale, changes are expected ranging from weeks, months, and years, out to those appearing as regional trends. The latter, in practice may be, just the expected oceanic response to past forcing—still "remembered" in the form of the continuing adjustment to the initial conditions.

To make this assertion more concrete, Fig. 7 shows one example of estimated northern hemisphere surface temperatures over the last 2000 years. Translating such a curve, even if taken at face value, into a rate of atmosphere-ocean heat-exchange is a major challenge. Nonetheless, for scaling purposes, suppose the approximately 0.2°C change over the last about 20 years corresponds to an exchange between ocean and atmosphere of 1 W/m^2. Then for example, the long decline from the year 1000 CE to about 1700 CE, if it too should correspond to 1 W/m^2, would imply a temperature reduction of about 35 times that estimated above for a 20-year interval. That reduction would then be overlain by the previous warming and then the rewarming over the past 300 years. Unless existing circulation rates have been grossly underestimated, the signature of the past state must be present in any measure of basin-scale and larger heat content or temperature shifts of the past few decades. No details are available, but discovering that parts of the system are still changing in ways unconnected to the recent increase in global average temperatures would not be a surprise.

Figure 7 here

The purpose of this paper is not the regional physics of thermal change. It is the summary estimation of the large regional changes in heat content, particularly in the abyss, as perceivable both as regional trend-like behavior on time-scales exceeding the 20-year estimate, and the superimposed higher frequency changes. These latter are both interesting in their own right, but also act as a noise in attempts to determine multi-decadal shifts. Regional dynamical interpretations as part of the generic problem of ocean "spin-up" is left for other studies.

3 Abyssal Signals

The eddy field in the ocean appears to be rich in the lowest baroclinic mode (Wunsch, 1997) and which implies a major eddy noise in the deep ocean. Study of the present eddy-free motions on time scales of less than about two years shows a strong coupling in both temperature and velocity between the upper and lower oceans, consistent with a primarily wind-forced response. Ponte (2012), using a different ECCO eddy-permitting (Menemenlis et al., 2005)—showed that abyssal noise could seriously compromise the interpretation of sea level variability, and hence heat content estimates at the levels of accuracy needed here.

Figure 8 here

Figure 9 here

Variances

The standard deviation of temperature variability at 2000 m is shown in Fig. 8—the central result here. For context, Fig. 9 is taken from the ECCO2, eddy-permitting state estimate of Menemenlis et al. (2005), used by Ponte (2012), and which shows the eddy noise variance (which is likely still underestimated owing to the 18 km horizontal resolution) is about six times larger than the background standard deviation. Also shown (Fig. 10) is the logarithm of the ratio of the eddy-permitting variances to that of the present state vector. The considerable eddy noise is obvious although indications exist of regions in which the eddy noise is smaller than the variance of the lower frequency shifts. Fig. 11 shows the standard deviation (without eddy noise) at 3600 m. Values at both 2000 m and 3600 m are small as compared to those in the thermocline. To move forward, the present analysis relies heavily on the assumption that the combination of constraints to observations and of the robust nature of the thermal wind relationships over long-distances, means that the state estimate faithfully tracks the large-scale thermal structures. The eddy field then represents a background noise primarily of concern in the noise-representing weights assigned to individual data points.

Figure 10 here

Figure 11 here

The most important result is that the standard deviation, or variance, pattern qualitatively replicates the tracer equilibrium time structure of Fig. 6. This structure is physically reasonable as regions functionally remote from atmospheric disturbances should show a muted response to short time-scale fluctuations as short-wavelength and high frequences are lost in propagation. Because the globally uniform boundary condition used for the passive tracer experiment is so different from those of atmospheric thermal disturbances, detailed resemblance is not expected.

Figure 12 here

Figure 13 here

Heat Content Regional Patterns

Heat content (J/m^2) between two depths z_1, z_2 at each horizontal location (θ, λ) is computed as,

$$H(z_1, z_2, \theta, \lambda, t) = \int_{z_2}^{z_1} c_p T(z, \theta, \lambda, t)\, dz,$$

where the heat capacity, $c_p = 3.8 \times 10^3$ J/kg/°C, is taken as a constant. Calculation with a spatially varying c_p changes nothing of significance here. Fig. 12 shows where heat is stored in the ocean, displaying the time-mean heat content, top-to-bottom, and Fig. 13 does so for the portion of the water column below 2000 m. The relatively warm North Atlantic and cold Southern and Pacific Oceans are apparent in both integrals. These patterns are important, because spatial gradients, both horizontal and vertical, are determinants of the future changes in these distributions. Regions of very small horizontal gradient cannot undergo future large temporal changes from advection or mixing except on very much longer time scales than the available 20 years.

To avoid discussion of the physical accuracy of a linear or other trend, Figs. 14–17 show the difference of the annual mean values 2011 minus 1993. 1992 is dropped as possibly showing signs of a starting transient. In the abyss, resemblances and differences to Fig. 6 can be seen. The western Atlantic and sectors of the deep Southern Ocean display a warming, with the remainder of the ocean either cooling (northwestern Indian Ocean, eastern basin of the Atlantic) or little or no change (the great bulk of the Pacific). Of most significance is the very strong regionality of the changes—expected from the numerous existing estimates of regional sea level variations.

Figure 14 here

Figure 15 here

Figure 16 here

Figure 17 here

At all depths, but particularly in the upper ocean, regions of warming are at least partially compensated in the global integrals by extended regions of cooling (especially the tropical Pacific and North Atlantic subtropical gyre). These patterns emphasize the the problem of having adequate spatial sampling to generate mean values consistent with the accuracies in Table 1.

Time Variations of Global Heat Content

The time variations of the spatially integrated values of H,

$$I_H\left(z_{1,}z_2,t\right)=\int\int_{ocean}H\left(z_1,z_2,\theta\,,\lambda,t\right)dA,$$

are shown in Fig. 18 for the integrals over varying depth ranges. The global integrals, reflecting the total ocean heat content and its changes are problematic relative to the regional changes, representing comparatively small residuals of much larger numbers. Nonetheless, with the continuing intense interest in determining net ocean heat uptake as a confirmation of estimates of radiative forcing changes, they are calculated here because they raise in a concrete fashion a number of measurement issues.

Figure 18 here

The timescale problem in models is greatly exacerbated by their known numerical drifts. ECCO state estimates have some immunity to this problem induced by the use of constraints forcing the model to those abyssal hydrographic data that do exist over the entire time interval, and by constraints preventing it from moving very far from the available crude climatologies. In addition, permitting comparatively slight adjustments in the model mixing parameters served to further reduce any tendency for the model to drift.

Near-surface and total values are dominated by the annual cycle. Although the annual cycle, and its sometimes important harmonics, is comparatively well-known—its large magnitude is important for the error budget of upper ocean measurements—as even small aliases, temporal or spatial, can mask lower frequency signals.

Figure 19 here

With the state estimate, removing the annual cycle, its first three harmonics, and the time-mean of the I_H is simple, and with the results shown in Figs. 19. A fit of a linear trend to the global integrals with a suppressed annual cycle in the I_H is also shown. In a formal sense, the apparent trends show a warming in the upper ocean and a net *cooling* below 2000 m. For $I_H\left(-3600,-h,t\right)$, the cooling is about 0.01°C over 19 years. As with many climate-related records, the unanswerable question here is whether these changes are truly secular, and/or a response to anthropogenic forcing, or whether they are instead fragments of a general rednoise behavior seen over durations much too short to depict the long time-scales of Fig. 6, 7, or the result of sampling and measurement biases, or changes in the temporal data density.

Time changes can sometimes be better estimated than the absolute accuracy. In the present cases, the temporal standard deviations, $\sigma_H\left(0,z\right)$, from monthly values over 20 years are displayed in Table 2 (including the annual cycles). A rough estimate of the formal accuracy with which a temporal change can be computed between any five year interval e.g., 1992-1996 versus 2006-2011, can be made by assuming that the five year average has a standard error of $\sigma_H/\sqrt{5}$, independent in the two intervals. (Because of the strong annual cycle, the monthly values are being assumed to be strongly correlated.) The difference between two estimates would have a formal standard error of $\sqrt{2\sigma_H^2/5}=.6\sigma_H$ or for the total, $H\left(0,-h,t\right)$, of 1.5×10^{22}J, heating equivalent over 20 years of 0.07 W/m^2 with a similar value for $H\left(0,-700\right)$. Note that the apparent "pause" in global ocean heat uptake since about 2004, documented e.g. by Lyman et al. (2010, their Fig. 2), amounts to about 4×10^{22} J in about 7 years. They show yearly 90% confidence intervals of 2-4×10^{22} J, roughly a heating error of 0.1 W/m^2, and consistent with those found here. Abyssal noise would contribute another 10% uncertainty to a water-column total. In any case, the small changes, including the pause, are at best at the very edge of what is practical precision today.

Table 2 here

The very important regional heterogeneity of change in heat content is obvious in the mapped figures. Temporal inhomogeneity is also considerable: Fig. 20 displays the detrended values of $H(-2000, -h, t)$ for a point in the eastern North Pacific, western North Atlantic and the Atlantic sector of the Southern Ocean at the locations listed. Detrending was done to avoid the question of the physical nature of the lowest frequency band. The Atlantic and Southern Ocean exhibit a great deal of excess high frequency energy relative to the eastern Pacific Ocean, confirmed in the spectra also shown in the figure. The eastern Pacific spectral estimate shows a "redder" structure, with lower energy at all frequencies. Return-time requirements for repeated sampling will evidently be different in different places.

Figure 20 here

In principle, a goal of 0.1 W/m^2 accuracy is within reach on a decadal basis from the state estimate without having to assume anything about the form of a trend. The reader is strongly cautioned, however, that this error estimate does not include any systematic errors that are likely present in the data and the model, nor the eddy-noise contribution. Meteorological forcing errors, mainly influencing the upper ocean on a 20-year time-scale, geothermal effects in the abyss, and initial condition errors representing on-going changes are only three of the many possibilities.

With all of the data available, the system is consistent with these comparatively small values of estimated heat-content, or equivalent volume averaged temperature, change. Of that total amount, approximately 10% is the contribution (a cooling) from below 2000 m—a value in accord with the global mean sea level contribution portion calculated by Ponte (2012) and consistent with the estimate of Kouketsu et al. (2011). It sets a limit to the precision to which an upper-ocean-alone estimate can be used to calculate the change in oceanic heat storage—*on this bidecadal time-interval*. In the active regions, the abyssal contribution is much larger than

10%, and what the future holds is unknown.

Comparison to Other Studies

A large number of studies from hydrographic data of abyssal changes with some overlap with this same period have been published, usually with reference to changes in a particular region. Representative among them are Bryden et al. (1996) for the North Atlantic at 24°N, Joyce et al. (1999) for the western North Atlantic, and Purkey and Johnson (2010) for the global ocean. In these three studies, at least some of the data used are part of the ECCO state estimate (data obtained in 1992 or later), but include observations preceding that period, typically the 1980s or the 1950s (from the Atlantic survey of the International Geophysical Year-IGY). With the caveat that abyssal changes from the 1980s and earlier need not be the same as those occurring later, and that temporally separated hydrographic sections are contaminated by aliasing, it is still useful to briefly compare the inferred changes with those in the state estimate.

Bryden et al. (1996) inferred a weak cooling of both basins of the North Atlantic at 24°N below 2000 m in the interval 1981-1992, just preceding the ECCO estimate time period. Their estimate for the longer interval 1957-1992 indicated a warming to about 3000 m with cooling below.

Joyce et al. (1999), working with two 1997 meridional sections in the western Atlantic at 52°and 66°W, compared them to nearly identical measurements in the mid-1980s and to the IGY. Although a lot of detail appears, and the changes in the two available time periods are different, they found a weak indication of warming between 2000 and 3000 m at most latitudes, more pronounced in the interval 1997-IGY. The patterns are very noisy, as the ECCO estimate shows, and a major change in measurement technology took place in the interim, but again no contradiction exists with the present results.

The Purkey and Johnson (2010) study is most directly relevant, as the bulk of their data are common to the ECCO estimate—coming from the WOCE period after 1992 and later. As with most such studies, one robust inference is that noise levels are high everywhere (e.g., their Fig. 6). A strong resemblance exists between their Fig. 8a (rendered as the heating at 4000 m in 24 regional basins, constituting about 10% of the ocean volume) and Fig. 17 here. Both depict warming in the abyss at high southern latitudes, in the western basin of the Atlantic and with cooling elsewhere. The consistency is at least reassuring, given that both studies used the same hydrographic data, but were carried out by completely different methods and with the state estimate employing a much larger and diverse data set. The latter is dominated by altimetry and upper ocean hydrography, but nonetheless tracks the abyssal hydrographic changes. Very different data sets are evidently qualitatively consistent.

The Kouketsu et al. (2011, hereafter K2011) estimation methodology is similar to ours: a GCM at 1° resolution and 46 vertical layers (version 3 of the GFDL/NOAA Modular Ocean Model, MOM3, Pacanowski and Griffies, 2000) was used in combination with temperature data to estimate abyssal warming. Among the numerous differences, apart from the model itself, are that they combined the Green function technique of Menemenlis et al. (2005) with the Lagrange multiplier method; only temperature and salinity data were used, but the denser global observing system observations including, Argo, satellite altimetry and scatterometry were omitted; the data sets extended back to 1985; and the computation was run over the 40 years beginning in 1957. In comparing their results to those of Purkey and Johnson (2010), K2011 used a much finer breakdown into 73 abyssal regions, presumably leaving a larger average residual noise level in each.

Given the numerous differences ranging from the model change to the very different data base (although the 1992-present hydrography would be common to both), it is unsurprising that the K2011 results differ in some ways from the present ones, but the similarities are significant.

They find regions below 3000 m of decadal scale cooling, confined primarily to the Indian Ocean and eastern North Atlantic. On the other hand, although parts of the Pacific Ocean between 3000 and 4000 m are estimated to have been cooling, in contrast with the present results, they showed a general warming below that, albeit rather weak between 4000 and 5000 m of roughly 2-3×10^{-3} °/decade, and with the region below 5000 m (which we have not separated out) showing considerable warming along with the general Southern Ocean. These numbers are sufficiently small that omission of the geothermal heating is a serious concern.

Distinguishing the differences between the various estimates becomes a complex problem in defining the systematic errors, which include the details of data sets used in each study, the assumed data and representation errors, and the residual misfits of the solutions. As noted repeatedly, the available data base is extremely limited, especially before 1992. The state-of-the-art does not permit resolving these differences. Hence, the main issue facing the oceanographic community is to obtain *future* data so that such ambiguities do not persist into the next several decades of change. A number of papers have appeared recently (e.g., Purkey and Johnson, 2013) focussing on changes in the Antarctic Bottom Water mass, and many discussions of other regional water mass property changes have also been published. A review of changes in individual water masses and varying depths and geography is beyond our present scope.

4 Sampling Without the Model

Most published estimates of oceanic heat content change have not employed a state estimate, but are generally described as being based upon the data alone and necessarily are commonly focussed on the upper ocean. As already noticed above, heating of the upper 700 m of the ocean by 1 W/m^2 for 20 years implies a temperature change of about 0.2°C as a water-column total. Although the upper ocean is not the focus here, an interesting and complex question whether the observational network is capable of producing estimates of small changes with a useful accuracy? Abraham et al. (2013) have described many of these calculations in detail and provide a list of references.

Some calculations have employed so-called empirical orthogonal functions (EOFs), or singular vectors, from models not unlike the one underlying the ECCO state estimate used here. These are the eigenvectors of the space-time correlation matrix of the model output used as an expansion basis. For example, the 240 monthly estimates from the present ECCO state estimates define 240 orthonormal vectors whose sum can perfectly reproduce either the global temperature at any depth or the heat content. Only 240 accurate measurements of the corresponding field would be adequate. As the number of data in each month tends to greatly exceed that value (see Fig. 21) obtaining high accuracy appears easy.

Figure 21 here

This description of the procedure is however, too facile. The correlation matrix eigenvectors are dependent upon the accuracy and stability of the matrix, as well as the differences in numerical values of the corresponding eigenvalues. Calculation of the resulting accuracy and stability from a finite time-duration involves the underlying spatially inhomogeneous, 4-dimensional space-time statistics of the state estimate. A major additional problem arises when those same eigenvectors are employed for time spans much exceeding that of the model or state-estimate duration—as the long oceanic memory implies ever-more physical regimes will come into play with longer times.

5 Discussion, With Comments on the Observation Problem

Bidecadal Abyssal Change

Over the 20 years of the present ECCO state estimate, changes in the deep ocean on multi-year time-scales are dominated by the western Atlantic basin and Southern Oceans. These are qualitatively consistent with expectations there of the comparatively rapid response to surface forcing. Defining the physics of those changes in terms of boundary currents, wave propagation, eddy-diffusion, and the myriad of other oceanic physical processes, region-by-region, remains a major unfinished piece of business. In those same regions, a longer-term general warming pattern occurs below 2000 m, interpreted here as owing to a disequilibrium of the abyssal ocean to the present atmosphere, with a superimposed multi-year noise. A very weak long-term cooling is seen over the bulk of the rest of the ocean below that depth, including the entirety of the Pacific and Indian Oceans, along with the eastern Atlantic Basin. The pattern below 3600 m is similar, with much smaller amplitude. These results differ in detail and in numerical values from other estimates, but the determining whether any are "correct" is probably not possible with the existing data sets.

The globally integrated heat content changes involve small differences of the much larger regional changes. As existing estimates of the anthropogenic forcing are now about $0.5\mathrm{W/m}^2$, the equivalent global ocean average temperature changes over 20 years are mostly slight compared to the shorter term temporal variations from numerous physical sources. Detailed attention must be paid to what might otherwise appear to be small errors in data calibration, and space-time sampling and model biases. Direct determination of changes in oceanic heat content over the last 20 years are not in conflict with estimates of the radiative forcing, but the uncertainties remain too large to rationalize e.g., the apparent "pause" in warming. The challenge is to develop observations so that future changes can be made with accuracies and precisions consistent with the conventional rule of thumb that they should be better than 10% of the expected signal.

Comments on Future Observations

No observing system can be designed and deployed that is capable of addressing all possible goals; specification of the particular purposes and the related accuracies and precisions is essential. Here the context of the discussion is (A) the global distribution by basin and, (B) directed at the problem of the determination of full water column changes in temperature (and salinity) over multiple decades. Although these choices are arbitrary to a degree, they address the important problems of sea level change and of ocean heat uptake, and are basic to classical scientific understanding of how the ocean varies through time and space. Absent a full optimization, a plausible strategy for moving forward is to concentrate abyssal samples where both the largest short-term signals are appearing (western basin of the Atlantic, the Southern Ocean) and with the highest noise levels, with only sporadic checks in the Pacific.

Ponte (2012) has summarized the abyssal measurement problem and its possibilities. Direct abyssal measurements by Argo profilers will likely become available in the next few years (D. Roemmich, personal communication, 2013). Acoustic tomographic measurements are another method for direct abyssal measurements. Satellite gravity data, such as are now available from the GRACE mission (Tapley, et al., 2004), produce estimates of the bottom pressure fluctuations. In discussions of how to ultimately construct a feasible and useful global-scale observing system by any or all means, it is essential to define the magnitude of the signals sought, and the structure in space and time of the noise field which tends to obscure those signals. Conceivably, a continuation of the existing hydrographic sampling is adequate for some purposes.

(Although not yet analyzed, calculated salinity changes are expected to display some resemblance to those for temperature, but not to be identical, as the relevant observing technology differs considerably, as do the boundary and initial conditions. With some additional effort, the ECCO state estimate can be used to calculate the structure of changes in other properties such as oxygen, carbon, silica, etc. and which are likely to be undergoing very different space and time evolution.)

That the noise level is also greatest (Figs. 8, 9) where the largest changes appear, is a challenge to any observing system. With a fuller understanding of the noise level, particularly of the abyssal eddy field, various strategies can be developed for basin-scale and global measurements of changing heat and, *mutatis mutandis*, the salinity and other fields. With growing confidence in the ECCO estimates, a practical strategy is to maintain a modestly augmented version of the existing observing system ("modest" in the sense of cost and ease of effort in sustaining it), and to focus on observational tests of the state estimate structures in crucial regions.

Acknowledgments.

Supported in part by the National Aeronautics and Space Administration and the National Ocean Partnership Program. We had useful comments from G. Forget, M. Tingley, P. Huybers, and two anonymous reviewers. The results rest on the efforts of members of the ECCO Consortium as a whole.

References

Adcroft, A., C. Hill, J-M. Campin, J. Marshall and P. Heimbach, 2004: Overview of the formulation and numerics of the MIT GCM. in: Proceedings of the ECMWF Seminar on "Recent developments in numerical methods for atmospheric and ocean modelling", 6-10 September 2004, Shinfield Park, Reading, UK, pp. 139-150,
http://www.ecmwf.int/publications/library/do/references/show?id=86400.

Abraham, J. P., and Coauthors, 2013: A review of global ocean temperature observations" implications for ocean heat content estimates and climate change. *Rev. Geophys.*, 51, 450-483.

Balmaseda, M. A., K. E. Trenberth, and E. Kallen, 2013: Distinctive climate signals in reanalysis of global ocean heat content. *Geophys. Res. Letts.*, 40, 1754-1759.

Bryden, H. L., M. J. Griffiths, A. M. Lavin, R. C. Millard, G. Parrilla,, and W. M. Smethie, 1996: Decadal changes in water mass characteristics at 24°N in the subtropical North Atlantic Ocean. *J. Climate*, 9, 3149-3161.

Chelton, D. B., and F. J. Wentz, 2005: Global microwave satellite observations of sea surface temperature for numerical weather prediction and climate research. *Bull. Amer. Meteor. Soc.*, 86, 1097-1115.

Church, J. A., et al., 2011: Revisiting the Earth's sea-level and energy budgets from 1961 to 2008. *Geophys. Res. Lett.*, 38(18). doi:10.1029/2011GL048794.

Dee, D. P., and Coauthors, 2011: The ERA-Interim reanalysis: configuration and performance of the data assimilation system. *Q. J. R. Meteorol. Soc.*, 137, 553-597.

Emile-Geay, J., and G. Madec, 2009: Geothermal heating, diapycnal mixing and the abyssal circulation. *Ocean Sci*, 5, 203-217.

Fenty, I.G. and P. Heimbach, 2013: Coupled Sea Ice-Ocean State Estimation in the Labrador Sea and Baffin Bay. *J. Phys. Oceanogr.*, 43(6), 884-904, doi:10.1175/JPO-D-12-065.1.

Ferreira, D., J. Marshall and P. Heimbach, 2005: Estimating eddy stresses by fitting dynamics to observations using a residual-mean ocean circulation model and its adjoint. *J. Phys. Oceanogr.*, 35(10), 1891-1910, doi:10.1175/JPO2785.1.

Hansen, J., and others, 2005: Earth's energy imbalance: confirmation and implications. *Science*, 308, 1431-1435.

Heimbach, P., C. Wunsch, R. M. Ponte, G. Forget, C. Hill, and J. Utke, 2011: Timescales and regions of the sensitivity of Atlantic meridional volume and heat transport magnitudes: Toward observing system design.. *Deep-Sea Res.-II*, 58, 1858-1879.

Huybers, P., and C. Wunsch, 2010: Paleophysical oceanography with an emphasis on transport rates. *Annu. Rev. Mar. Sci.*, 2, 1-34.

Joyce, T. M., R. S. Pickart, and R. C. Millard, 1999: Long-term hydrographic changes at 52 and 66 degrees W in the North Atlantic Subtropical Gyre & Caribbean. *Deep-Sea Res.* II, 46, 245-278.

Kosaka, Y. and S.-P. Xie, S.-P., 2013: Recent global-warming hiatus tied to equatorial Pacific surface cooling. *Nature*, 501(7467), 403407. doi:10.1038/nature12534.

Kouketsu, S., and Coauthors, 2011: Deep ocean heat content changes estimated from observation and reanalysis product and their influence on sea level change. *J. Geophys. Res.*, 116, C03012 DOI: 10.1029/2010JC006464.

Ljungqvist, F. C., 2010: A new reconstruction of temperature variability in the extra-tropical northern hemisphere during the last two millennia. *Geografiska Annaler*, 92(A), 339-351.

Losch, M., D. Menemenlis, J.M. Campin, P. Heimbach, and C. Hill, 2010: On the formulation of sea-ice models. Part 1: Effects of different solver implementations and parameterizations. *Ocean Modelling*, 33(1-2), 129-144, doi:10.1016/j.ocemod.2009.12.008.

Lyman, J. M., and Coauthors, 2010: Robust warming of the global upper ocean. *Nature*, 465, 334-337.

Marshall, J., A. Adcroft, C. Hill, L. Perelman, and C. Heisey, 1997: A finite-volume, incompressible Navier Stokes model for studies of the ocean on parallel computers. *J. Geophys. Res.-Oceans*, 102, 5753-5766.

Menemenlis, D., and Coauthors, 2005: NASA supercomputer improves prospects for ocean climate research. *Eos,* 86(9).

Pacanowski, R. C., and S. M. Griffies, 2000: The Modular Ocean Model (MOM) 3 Manual, technical document. Geophysical Fluid Dynamics Laboratory (GFDL), Princeton, N. J.

Peacock, S., and M. Maltrud, 2006: Transit-time distributions in a global ocean model. *J. Phys. Oceanogr.*, 36, 474-495.

Pollack, H. N., S. J. Hurtrer, and J. R. Johnson, 1993: Heat flow from the Earth' s interior: analysis of the global data set. *Rev. Geophys.*, 31, 267-280.

Ponte, R. M., 2012: An assessment of deep steric height variability over the global ocean. *Geophys. Res. Letts.*, 39, L04601.

Purkey, S. G., and G. C. Johnson, 2010: Warming of global abyssal and deep Southern Ocean Waters between the 1990s and 2000s: Contributions to global heat and sea level rise budgets. *J. Climate*, 23, 6336-6351.

Purkey, S. G. and G. C. Johnson, 2013: Antarctic Bottom Water warming and freshening: contributions to sea level rise, ocean freshwater budgets, and global heat gain. *J. Climate*, 26, 6105-6122.

Reynolds, R. W., T. M. Smith, C. Liu, D. B. Chelton, K. S. Casey, and M. G. Schlax, 2007: Daily high-resolution-blended analyses for sea surface temperature. *J. Climate*, 20, 5473-5496.

Roemmich, D., and C. Wunsch, 1984: Apparent change in the climatic state of the deep North Atlantic Ocean. *Nature*, 307, 447-450.

Roemmich, D., W. John Gould, and J. Gilson, 2012: 135 years of global ocean warming between the Challenger expedition and the Argo Programme. *Nature Clim. Change*, 2, 425-428.

Roemmich, D., and Coauthors, 2009: The Argo Program observing the global ocean with profiling floats. *Oceanography*, 22, 34-43.

Roquet, F., and a. Coauthors, 2013: Hydrographic data collected by seals significantly reduce the observational gap in the Southern Ocean. *Geophys. Res. Letts.*, in press.

Talley, L. D., 2007: *Hydrographic Atlas of the World Ocean Circulation Experiment (WOCE) Volume 2: Pacific Ocean* (Eds. M. Sparrow, P. Chapman, and J. Gould). http://www-pord.ucsd.edu/whp.mscatlas/pacific.mscindex.htm.

Tapley, B. D., S. Bettadpur, J. C. Ries, P. F. Thompson, and M. M. Watkins, 2004: GRACE measurements of mass variability in the Earth system. *Science*, 305, 503-505.

von Schuckmann, K., and P.-Y. Le Traon, 2011: How well can we derive Global Ocean Indicators from Argo data?, *Ocean Sci.*, 7, 783-791, doi:10.5194/os-7-783-2011.

Worthington, L.V., 1981: The water masses of the world ocean: some results of a fine-scale census. In: Warren, B.A. and C. Wunsch (Eds.): Evolution of Physical Oceanography, Scientific Surveys in Honor of Henry Stommel. MIT Press, Cambridge, MA, pp. 4269.

Wunsch, C., 1997: The vertical partition of oceanic horizontal kinetic energy. *J. Phys. Oceanogr.*, 27, 1770-1794.

Wunsch, C., and P. Heimbach, 2007: Practical global oceanic state estimation. *Physica D-Nonlinear Phenomena*, 230, 197-208.

Wunsch, C., and P. Heimbach, 2008: How long to ocean tracer and proxy equilibrium? *Quat. Sci. Rev.*, 27, 1639-1653.

Wunsch, C., and P. Heimbach, 2013a: Dynamically and kinematically consistent global ocean circulation state estimates with land and sea ice. In *Ocean Circulation and Climate*, 2nd Edition, J. C. G. Siedler, W. J. Gould, S. M. Griffies, Eds., pp. 553-579, Elsevier.

Wunsch, C., and P. Heimbach, 2013b: Two decades of the Atlantic meridional overturning circulation: anatomy, variations, extremes, prediction, and overcoming its limitations. *J. Climate*, 26, 7167-7186.

Figure Captions

1. Hydrographic data reaching to 2000 m betweeen 1992 and 2000 (a) and between 2001 and 2011 (b). The lower two panels (c,d) are the corresponding distributions reaching at least to 3600 m in the same two intervals.

2. The standard deviation of temperature in the grid cells, in space and time over 20 years, in the state estimate domain as a function of depth (solid line). In the absence of the eddy field, this curve is a very optimistic basis for determining average temperatures. Not area weighted. The variance includes the spatial time-mean contribution, which strongly dominates. The ability to remove it accurately is an issue in computing time-changes from direct point observations. The dashed line is the global mean standard deviation of the annual component.

3. Volumetric census—cubic meters of water lying in fixed intervals of temperature and salinity—of the state estimate in 1993 in logarithmic units. Total volume is about $1.3\times10^{18}\mathrm{m}^3$. The mean value is shown by 'o' at 3.5°C and 34.8. Worthington (1981) reported a mean of 3.5°C and 34.7‰ on the basis of an ocean he optimistically regarded as 46% sampled. A 1 W/m^2 net oceanic heating would shift the mean temperature by approximately 0.04°C in 20 years showing the necessity of observation of the massive cold abyssal water masses.

4. Mean differences in °C between the CTD data and the state estimate as a function of depth. In the state estimate, these squared deviations are normalized by the expected errors and which on average should be consistent with a χ_2^2 distribution with mean near unity.

5. As in Fig. 4 for the mean model minus CTD data in °C in abyss (below 2000 m).

6. Time in years for a passive tracer to reach 90% of its equilibrium value at 2000 m when a globally uniform concentration is imposed at the sea surface and held there (from Wunsch

and Heimbach, 2008). These values can be interpreted as a measure of the ocean memory and which ranges, at this depth, from several hundreds to several thousands of years. Extrapolation of the 1900 year computation was used to estimate the much longer North Pacific equilibrium times. Note that an active tracer—one such as temperature modifying density—would have a different history, generating faster baroclinic disturbances, but the regional time histories will again extend over very long time-intervals.

7. An estimate used here for scaling purposes (Ljunqvist, 2010) of northern hemisphere surface temperatures (ocean and land) dating to 1 CE (AD in the figure) showing multidecadal and much longer intervals of warmer and colder temperatures. The medieval warm period and the Little Ice Age are conspicuous. Gray band is the estimated two standard deviation uncertainty (likely optimistic). If translatable into air-sea heat transfers (by no means clear) then the ocean should today retain a memory of these past states as the time scales in Fig. 6 exceed this duration.

8. Base 10 logarithm of the standard deviation from monthly averages of temperature at 2000 m in the state estimate. Atlantic and Southern Oceans carry most of the variability.

9. Estimated base 10 log of the standard deviation of temperature at 2000 m in the eddy-permitting ECCO2 state estimate. Variability on scales larger than about 3° of latitude and longitude was suppressed to approximately isolate the synoptic eddy-scale contribution.

10. Base 10 logarithm of the ratio of the variance of the ECCO2 temperature variations near 2000 m (scales shorter than about 3° of latitude and longitude) to that in the version 4 state estimate without eddies. The spatial average eddy contribution is approximately 6 times the ECCO estimated variance. Regions with a logarithm below 0 are places where the interannual

variability appears to exceed the eddy noise and would be of great observational significance if ocean warming were expected to be globally uniform.

11. Same as Fig. 8 except at 3600 m. Note that the high southern latitudes have become the most active regions at this depth, in contrast to the behavior nearer the sea surface.

12. Heat content, $H(0,-h)$, in the time mean, top-to-bottom using °C. Notice the strong meridional gradients at high latitudes. White contour is the boundary of mean negative temperatures and thus apparent negative heat content using a Celsius temperature scale. The relatively large heat content of the Atlantic Ocean could, if redistributed, produce large changes elsewhere in the system and which, if not uniformly observed, would show artificial changes in the global average.

13. Time mean heat content below 2000 m, $H(2000,-h)$. The warmer Atlantic remains visible at these depths. Weak gradients in the Pacific would minimize any observed time changes owing to lateral motions or diffusion. White contour is again the boundary of zero mean temperatures.

14. Difference in heat content of the annual average of 2011 minus that of 1993, $H(0,-h,2011)-H(0,-h,1993)$. The strong spatial structure represents a major observational challenge to determining an accurate mean change. A conspicuous cooling of the eastern Pacific Ocean has been the subject of various speculative scenarios (e.g., Kosaka and Xie, 2013).

15. Same as Fig. 14 except for the top 700 m alone, $H(0,-700,2011)-H(0,-700,1993)$. Annual cycle and harmonics removed. Regions of loss as well as gain depict some of the sampling difficulty.

16. Same as Fig. 14 except for 2000 m to the bottom.

17. Same as Fig. 14 except for 3600 m to the bottom. Note the cooling in the deepest parts of the western North Atlantic, the entire eastern basin, Pacific and Indian Oceans. Warming of the Antarctic Bottom Water has been discussed recently by Purkey and Johnson (2013) among others. In the present context, it is a comparatively small water mass. Warming in the Atlantic sector Southern Ocean is particularly conspicuous.

18. Time variability of the globally integrated $H(z=0,z_j,t)$ and denoted $I_H(z_1,z_2,t)$ as labelled, $I_H(0,-100,t)$, $I_H(0,-700,t)$, $I_H(-2000,-h,t)$, $I_H(-3600,-h,t)$ and the top-to-bottom integral $I_H(0,-h,t)$. In Yotta Joules (YJ $= 10^{24}$ J). A change of 0.1 YJ over the mean water depth of 3700 m corresponds to a temperature change of about 0.02°C.

19. The same as Fig. 18 except the annual cycle has been removed. Dashed-dot lines are the best linear fits, and dashed lines are the residual. The 1997-1998 ENSO event is visible primarily in $I_H(0,-100,t)$, but can also be detected below, where the thermal anomaly is largely compensated. Because of the very long time scales embedded in the oceans, and the very great spatial structure, no particular significance is attached here to the apparent linear trends where visible, as they may well be fragments of much longer rednoise trends or systematic errors.

20. (Upper panel) Time series of $H(-2000,-h,t)$ from the eastern Pacific (sold curve), the western Atlantic (dashed curve, and the Southern Ocean (dotted). . (Lower panel) Power density spectral estimates for the three records shown above. All records approach white noise at low frequencies beyond about 10 years period, with an order of magnitude less variance in the Pacific Ocean. The power laws at high frequencies, s, lie between about -2.2 to -3, although that characterization is over-simplified. Note that multitaper spectral methods are biassed low at the longest periods. Vertical bar is an approximate 95% confidence interval.

21. Number of observations extending below 2000 m for each year (solid curve) and below

3600 m (dashed). Upper ocean observations (not shown) greatly increase with the Argo array from the middle 2000s, introducing an important inhomogeneity with time in the estimates.

Table Captions

Table 1. Approximate oceanic temperature changes implied by a 1 W/m^2 heating-rate over different times and depths, as well as the temperature change equivalent of a 1 mm/y global mean sea level (GMSL) change.

Table 2. Standard deviation of the total heat content between the depths indicated from the 20-year state estimate, and of the equivalent heating rate over 20 years.

Period & Fraction of Water Column	**1 W/m^2 Heating rate**	**1 mm/y GMSL change**
1 Year, Full Depth	0.002°C	0.0015°C
20 Years, Full Depth	0.04°C	0.03°C
1 Year, Upper 700 m	0.01°C	0.008°C
20 Years, Upper 700 m	0.2°C	0.16°C
1 Year, Below 700 m	0.0025°C	0.002°C
20 Years, Below 700 m	0.05°C	0.04°C

Table 1: Approximate oceanic temperature changes implied by a 1 W/m^2 heating-rate over different times and depths, as well as the temperature change equivalent of a 1 mm/y global mean sea level (GMSL) change.

{table1}

	0 to h	0 to 100 m	0 to 700 m	2000 m to h	3600 m to h
Energy, 10^{22}J	2.4	1.8	2.4	0.33	0.39
Rate/20 y, W/m^2	0.11	0.08	0.11	0.01	0.02

Table 2: Standard deviation of the total heat content between the depths indicated from the 20-year state estimate, and of the equivalant heating rate over 20 years.

{table2}

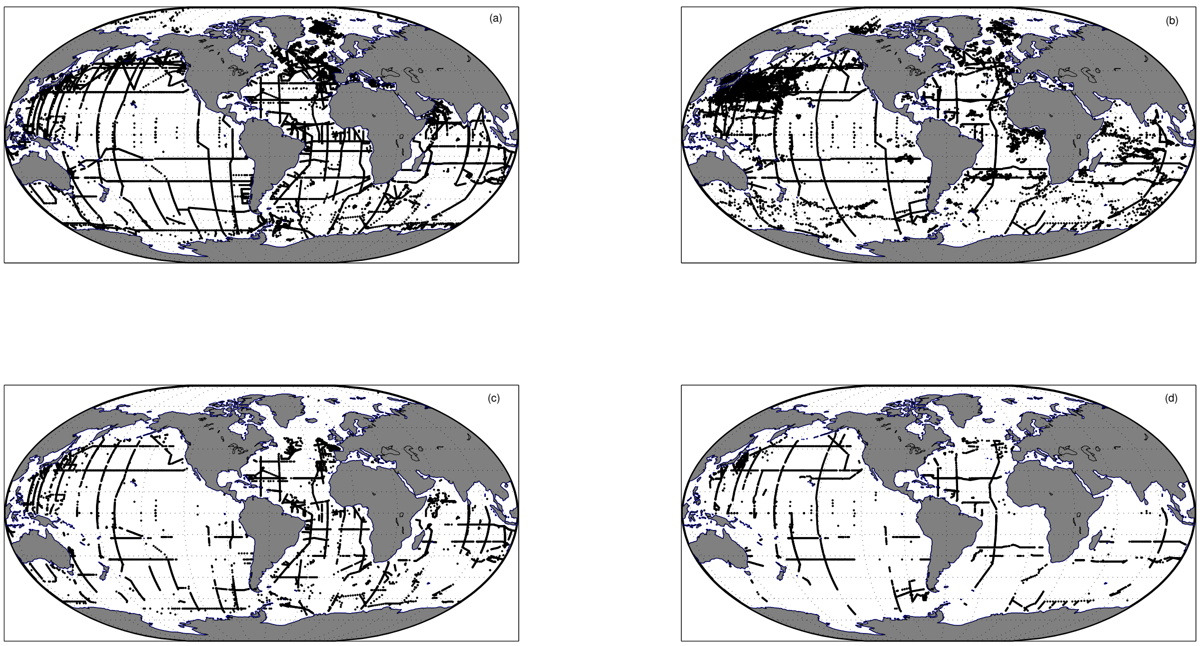

Figure 1: Hydrographic data reaching to 2000 m betweeen 1992 and 2000 (a) and between 2001 and 2011 (b). The lower two panels (c,d) are the corresponding distributions reaching at least to 3600 m in the same two intervals.

{data_dist_200

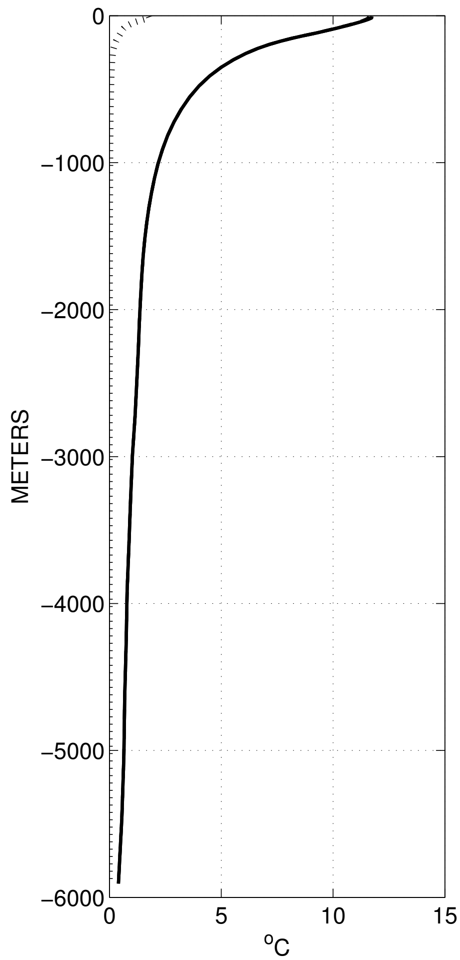

Figure 2: The standard deviation of temperature in the grid cells, in space and time over 20 years, in the state estimate domain as a function of depth (solid line). In the absence of the eddy field, this curve is a very optimistic basis for determining average temperatures. Not area weighted. The variance includes the spatial time-mean contribution and which strongly dominates. The ability to remove it accurately is an issue in computing time-changes from direct point observations. The dashed line is the global mean standard deviation of the annual component.

{temper_stddev

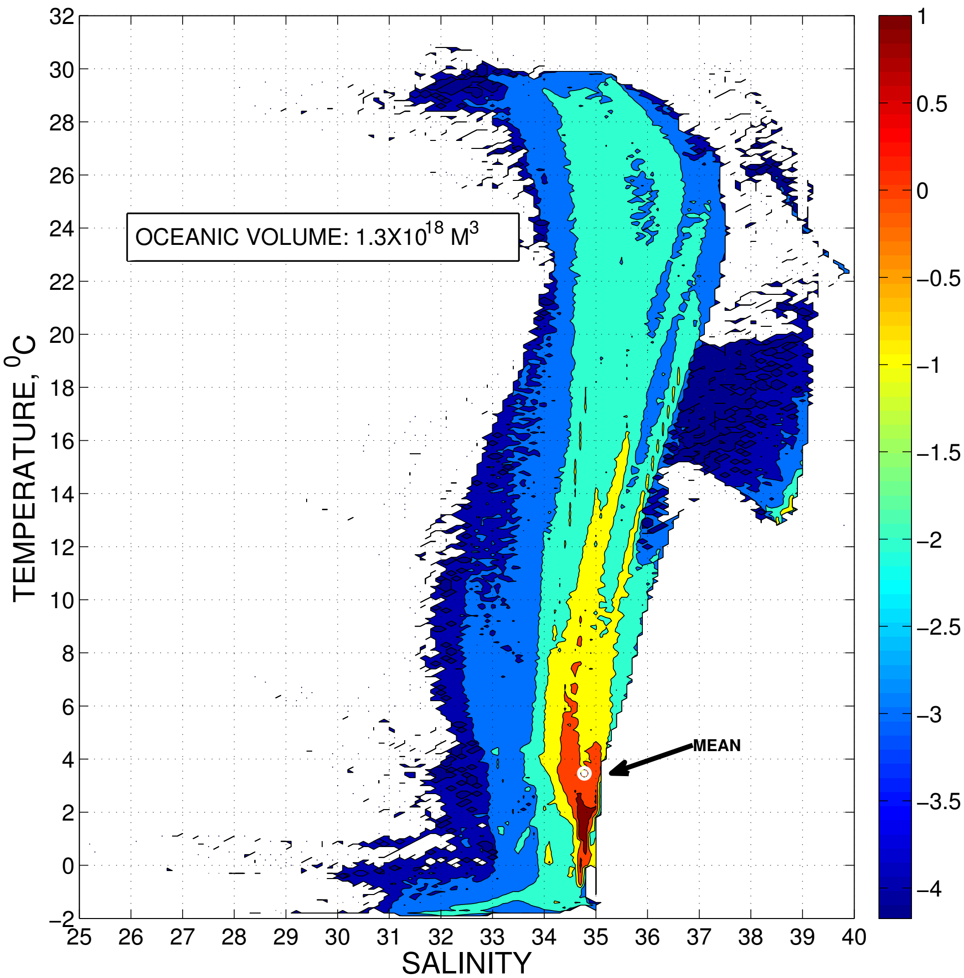

Figure 3: Volumetric census—cubic meters of water lying in fixed intervals of temperature and salinity—of the state estimate in 1993 in logarithmic units. Total volume is about $1.3 \times 10^{18}\mathrm{m}^3$. The mean value is shown by 'o' at 3.5°C and 34.8. Worthington (1981) reported a mean of 3.5°C and 34.7‰ on the basis of an ocean he optimisitcally regarded as 46% sampled. A 1 $\mathrm{W/m}^2$ net oceanic heating would shift the mean temperature by approximately 0.04°C in 20 years showing the necessity of observation of the massive cold abyssal water masses.

{hist_2d_ver4.

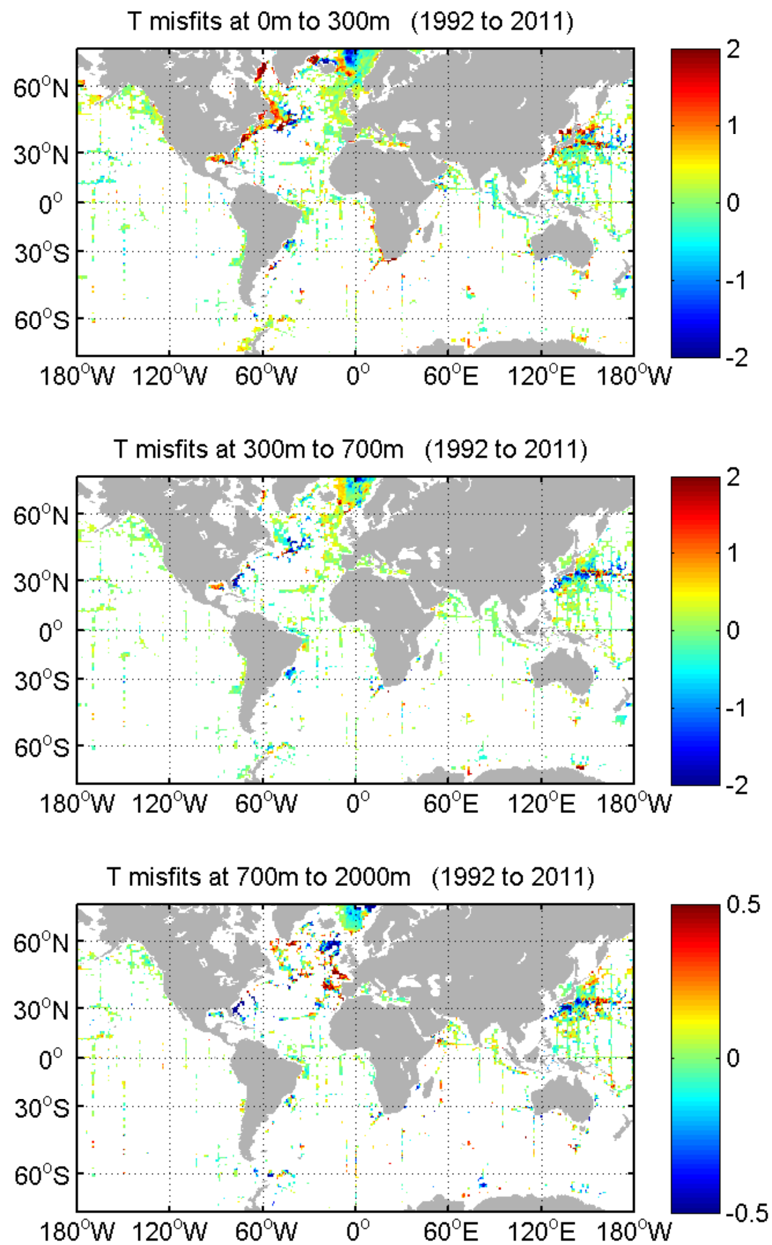

Figure 4: Mean differences in °C to the CTD data in the state estimate as a function of depth. In the state estimate, these squared deviations are normalized by the expected errors and which on average should be consistent with a χ^2 distribution with mean near unity.

{insitu_misfit

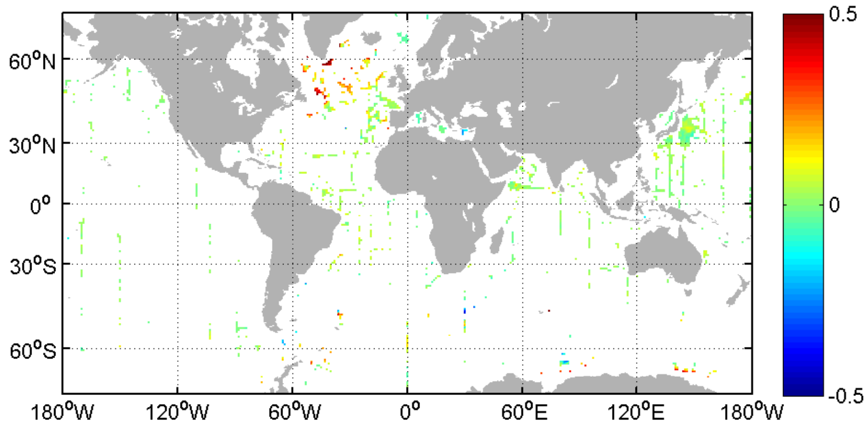

Figure 5: As in Fig. 4 for the mean model minus CTD data in °C in abyss (below 2000 m). {insitu_misfit

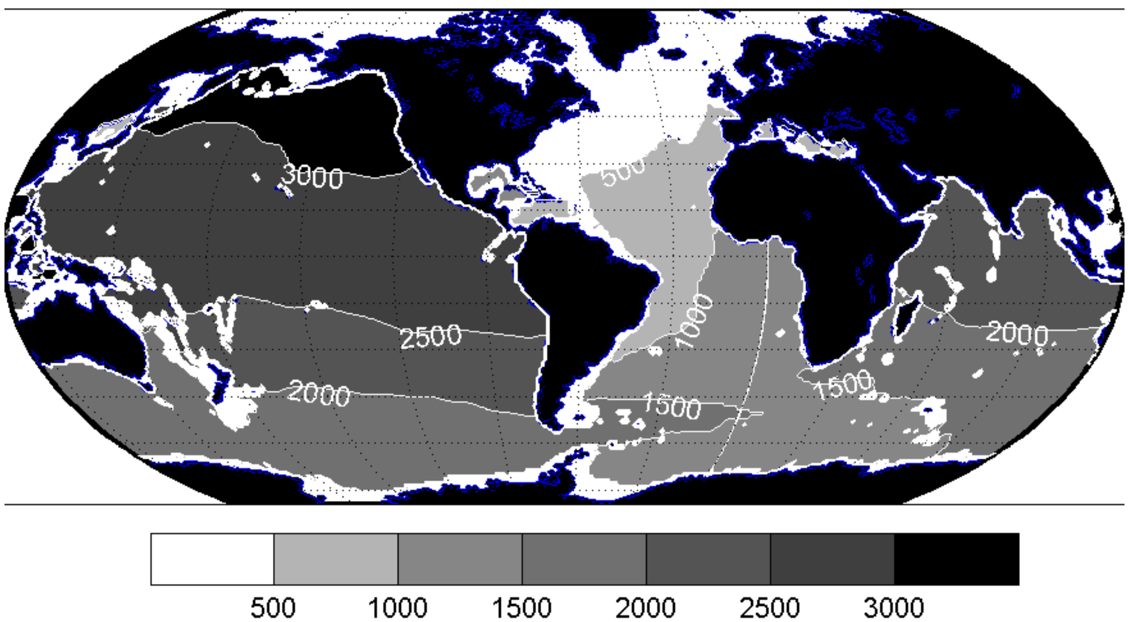

Figure 6: Time in years for a passive tracer to reach 90% of its equilibrium value at 2000 m when a globally uniform concentration is imposed at the sea surface and held there (from Wunsch and Heimbach, 2008). These values can be interpreted as a measure of the ocean memory, which ranges, at this depth, from several hundreds to several thousands of years. Extrapolation of the 1900 year computation was used to estimate the much longer North Pacific equilibrium times. Note that an active tracer—one such as temperature modifying density —would have a different history, generating faster baroclinic disturbances, but final equilibrium will again likely be diffusively controlled.

{global1975_eq

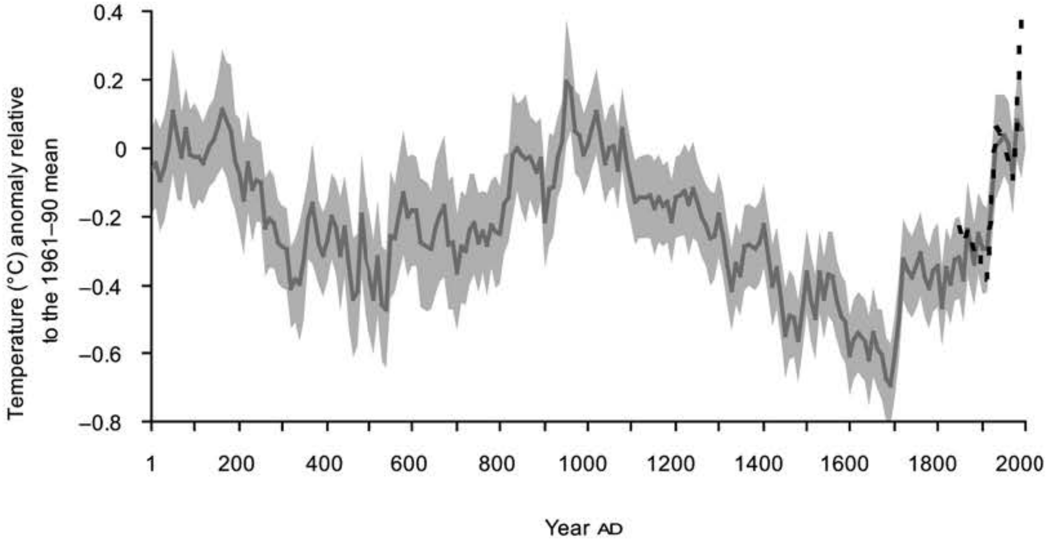

Figure 7: An estimate used here only for scaling purposes (Ljunqvist, 2010) of northern hemisphere surface temperatures (ocean and land) dating to 1 CE (AD in the figure) showing multidecadal and much longer intervals of warmer and colder temperatures. The medieval warm period and the Little Ice Age are conspicuous. Gray band is the estimated two standard deviation uncertainty (likely optimistic). If translatable into air-sea heat transfers (by no means clear) then the ocean should today retain a memory of these past states as the time scales in Fig. 6 exceed this duration. {ljunquist_mil

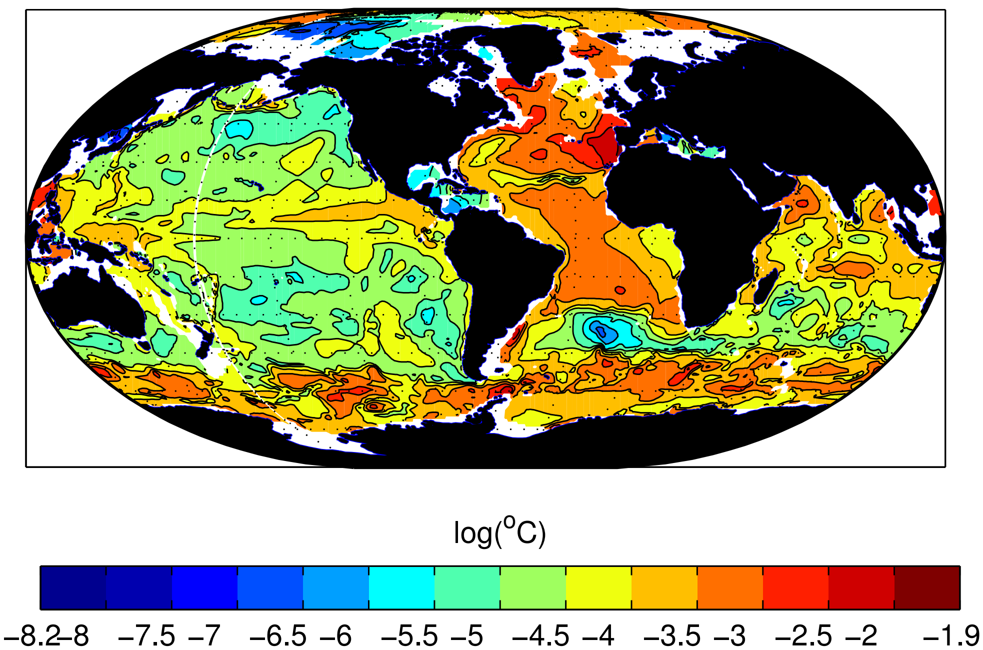

Figure 8: Base 10 logarithm of the standard deviation from monthly averages of temperature at 2000 m in the state estimate. Atlantic and Southern Oceans carry most of the variability. {temper_stddev

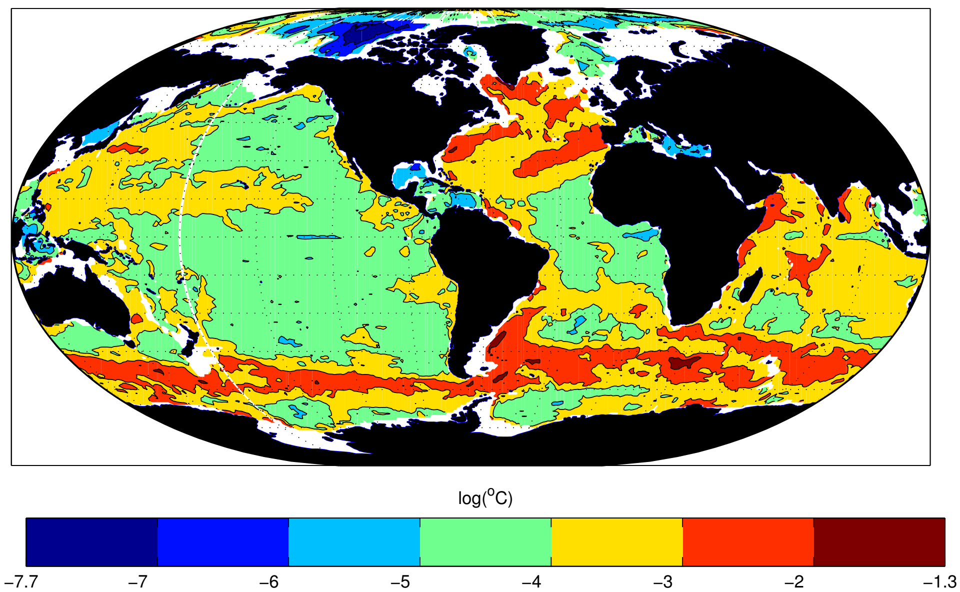

Figure 9: Estimated base 10 log of the standard deviation of temperature at 2000 m in the eddy-permitting ECCO2 state estimate. Variability on scales larger than about 3° of latitude and longitude was suppressed to approximately isolate the synoptic eddy-scale contribution. {logstdev2000m

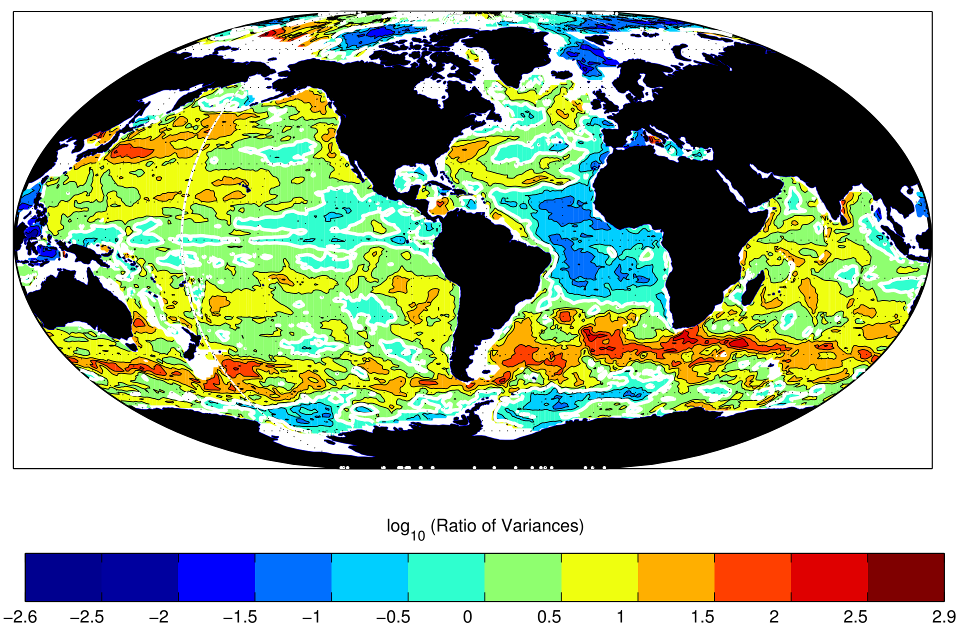

Figure 10: Base 10 logarithm of the ratio of the variance of the ECCO2 temperature variations near 2000 m (scales shorter than about 3° of latitude and longitude) to that in the version 4 state estimate without eddies. The spatial average eddy contribution is approximately 6 times the ECCO estimated variance. Regions with a logarithm below 0 are places where the interannual variability appears to exceed the eddy noise and would be of great observational significance if ocean warming expected to be globally uniform.

{temper_varian

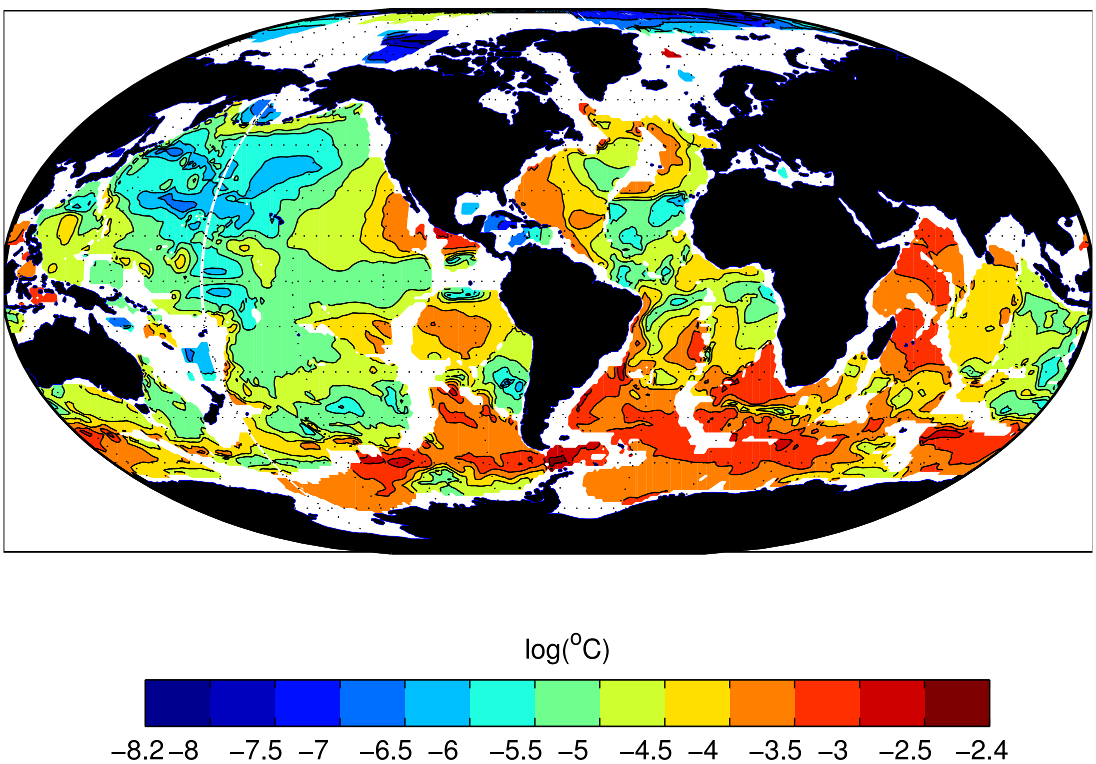

Figure 11: Same as Fig. 8 except at 3600 m. Note that the high southern latitudes have become the most active regions at this depth, in contrast to the behavior nearer the sea surface. {temper_stddev

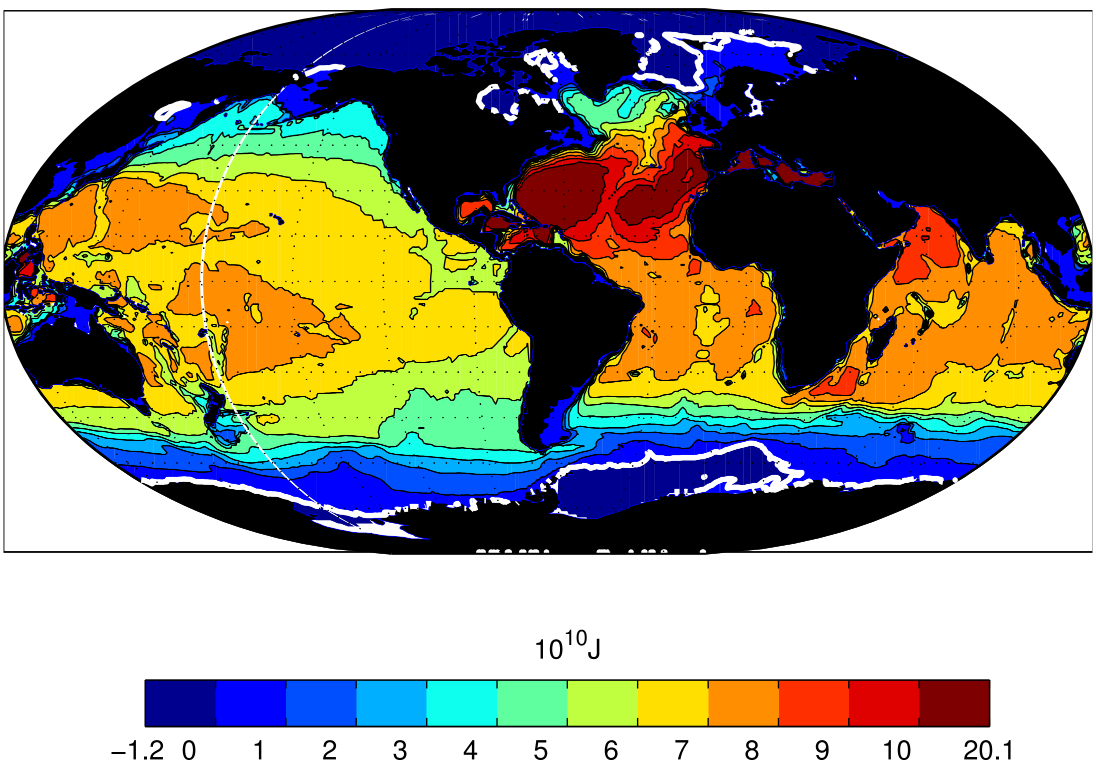

Figure 12: Heat content, $H(0,-h)$, in the time mean, top-to-bottom using °C. Notice the strong meridional gradients at high latitudes. White contour is the boundary of mean negative temperatures and thus apparent negative heat content using a Celsius temperature scale. The relatively large heat content of the Atlantic Ocean could, if redistributed, produce large changes elsewhere in the system and which, if not uniformly observed, show artificial changes in the global average. {htot_timemean

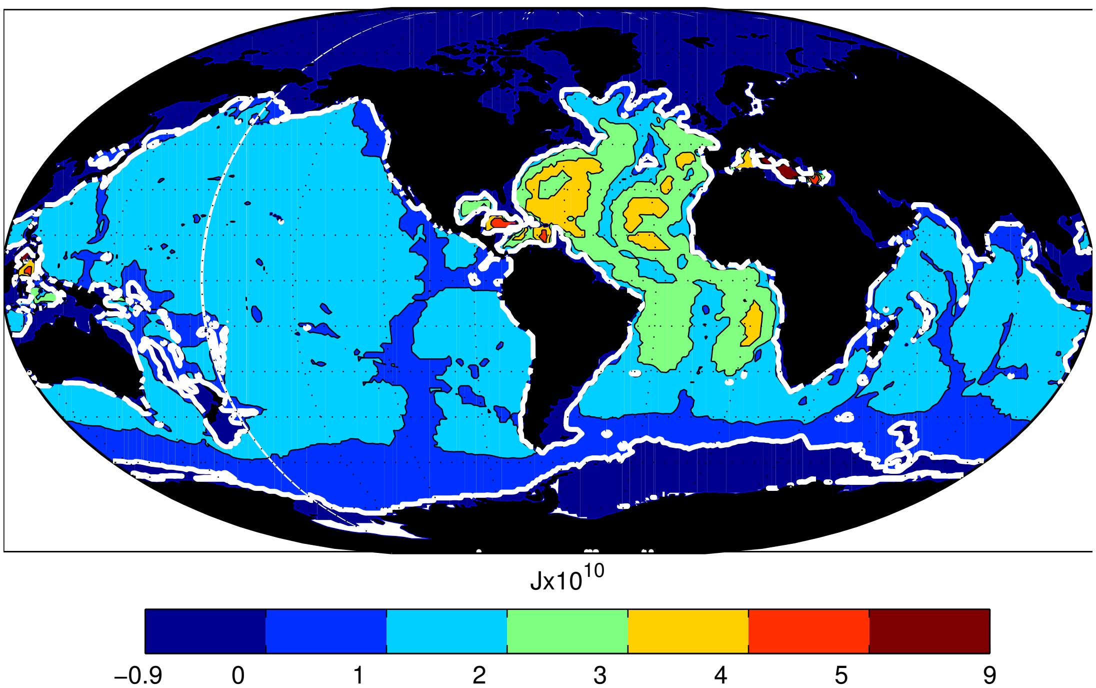

Figure 13: Time mean heat content below 2000 m, $H(2000, -h)$. The warmer Atlantic remains visible at these depths. Weak gradients in the Pacific would minimize any observed time changes owing to lateral motions or diffusion. White contour is again the boundary of zero mean temperatures. {h2000m_timeme

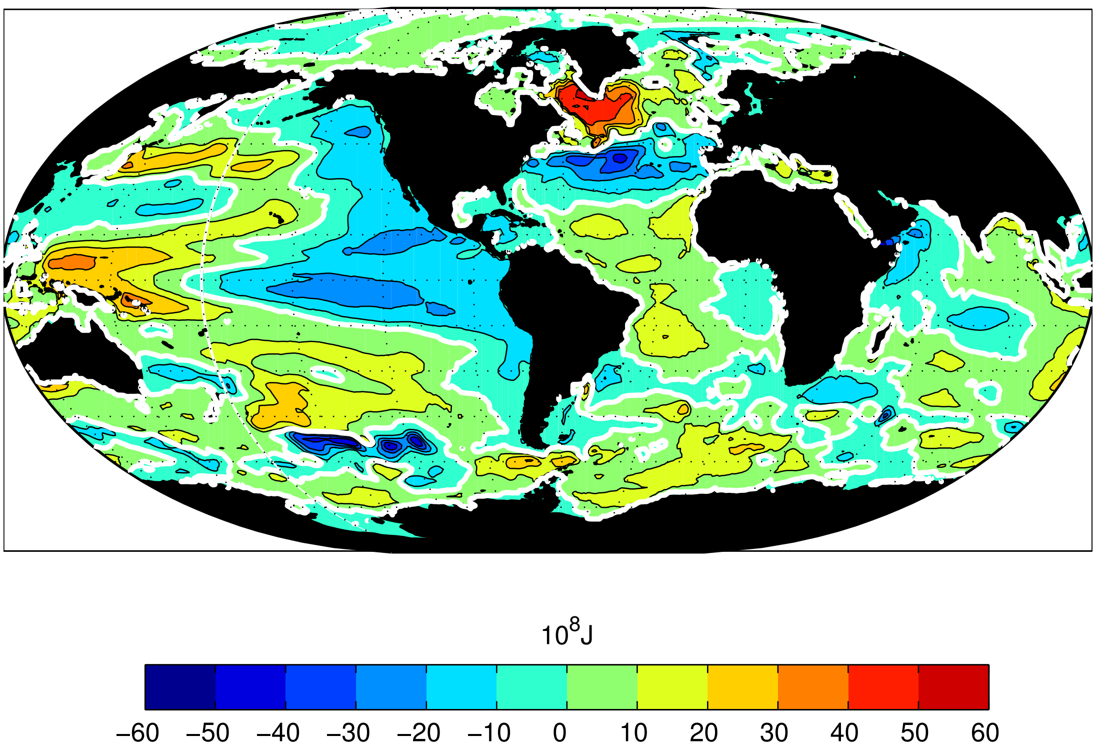

Figure 14: Difference in heat content of the annual average of 2011 minus that of 1993, $H(0,-h,2011) - H(0,-h,1993)$. The strong spatial structure represents a major observational challenge to determining an accurate mean change.

{htot_change.e

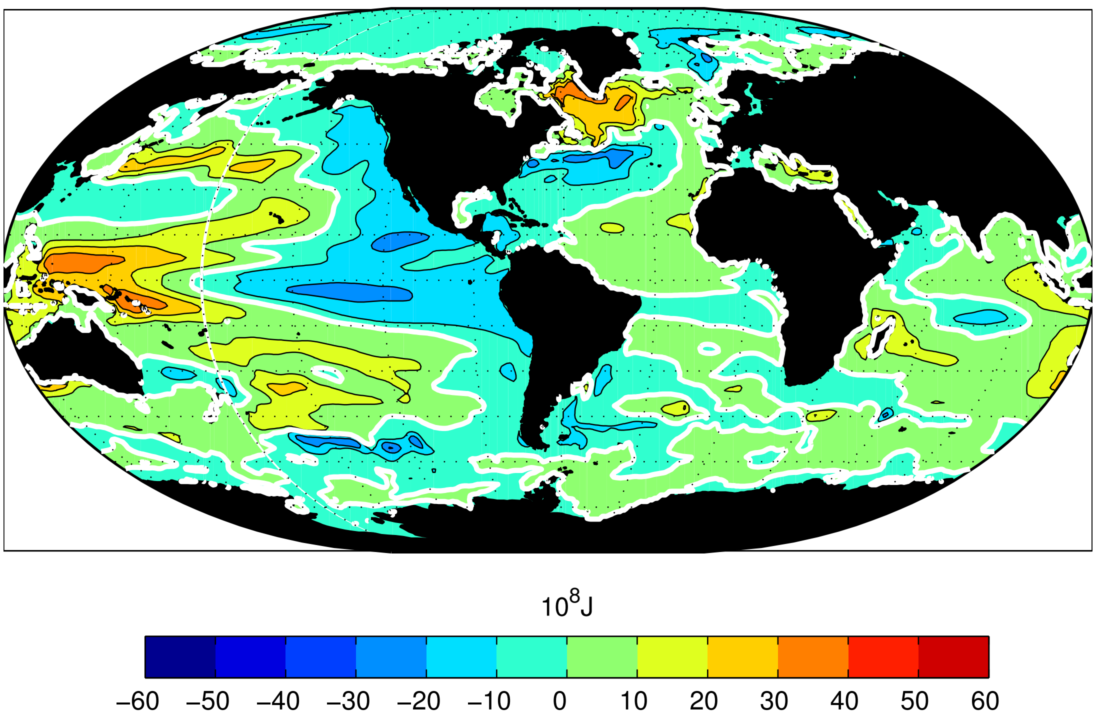

Figure 15: Same as Fig. 14 except for the top 700 m alone, $H(0, -700, 2011) - H(0, -700, 1993)$. Annual cycle and harmonics removed. Regions of loss as well as gain depict some of the sampling difficulty. {h700m_change.

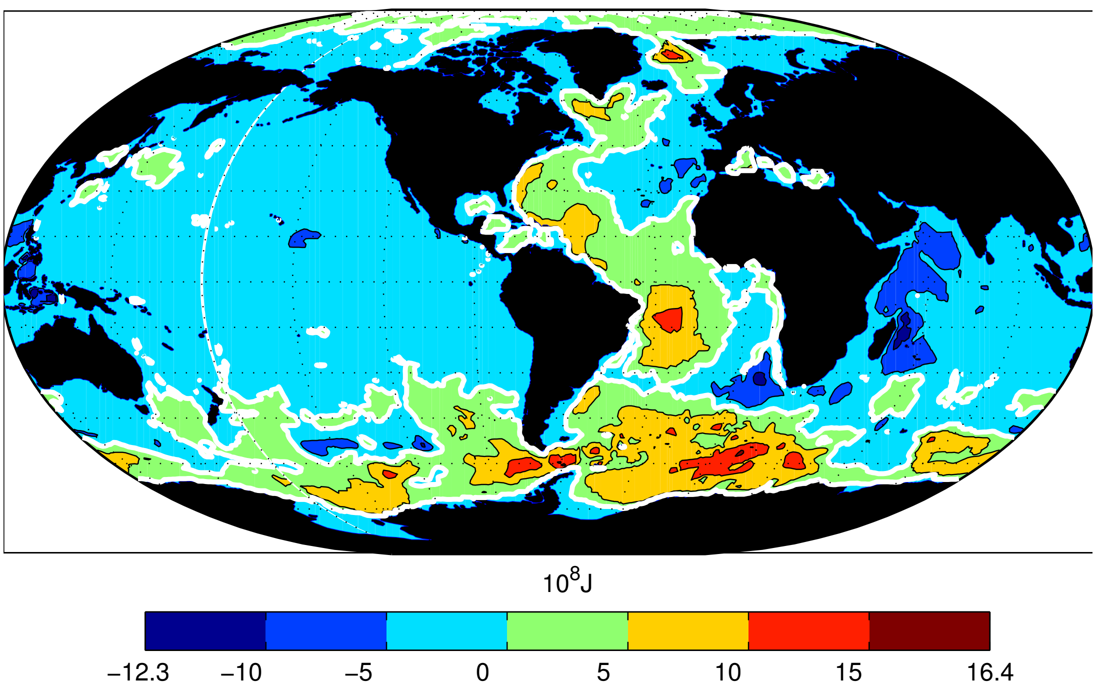

Figure 16: Same as Fig. 14 except for 2000 m to the bottom.

{h2000m_change

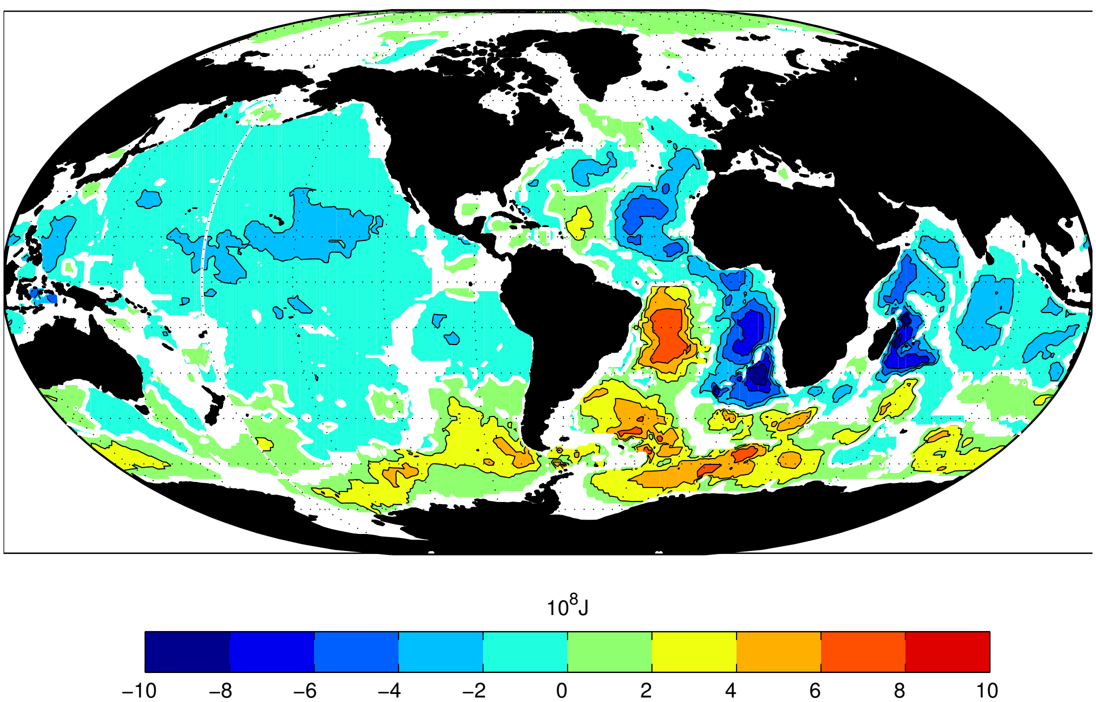

Figure 17: Same as Fig. 14 except for 3600 m to the bottom. Note the cooling in the deepest parts of the western North Atlantic, the entire eastern basin, Pacific and Indian Oceans. Warming of the Antarctic Bottom Water has been discussed recently by Purkey and Johnson (2013) among others. In the present context, it is a comparatively small water mass. Warming in the Atlantic sector Southern Ocean is particularly conspicuous.

{h3600m_change

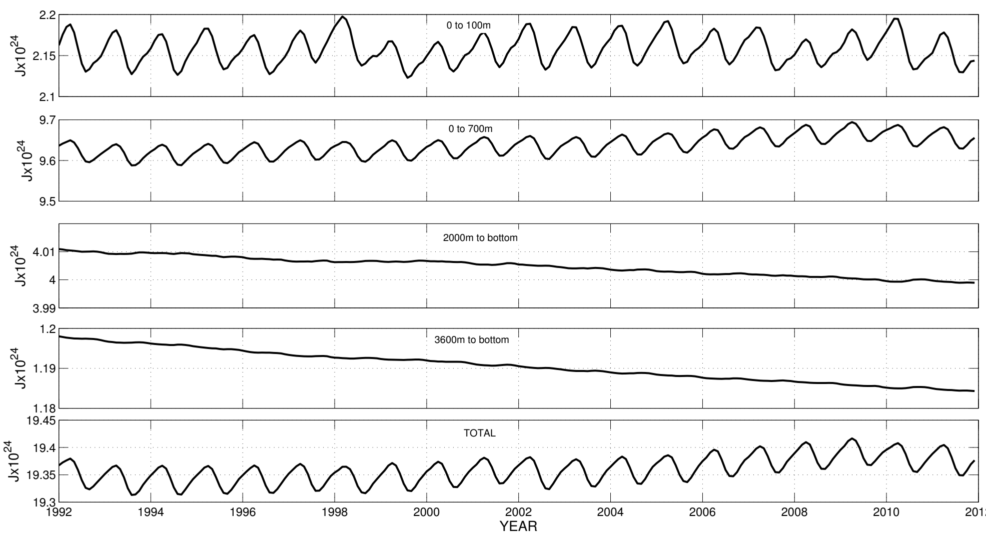

Figure 18: Time variability of the globally integrated $H\,(z=0, z_j, t)$ and denoted $I_H\,(z_1, z_2, t)$ as labelled, $I_H(0, -100, t)$, $I_H(0, -700, t)$, $I_H(-2000, -h, t)$, $I_H\,(-3600, -h, t)$ and the top-to-bottom integral $I_H(0, -h, t)$. In Yotta Joules (YJ $= 10^{24}$ J). A change of 0.1 YJ over the mean water depth of 3700 m corresponds to a temperature change of about 0.02°C.

{h_ts.eps}

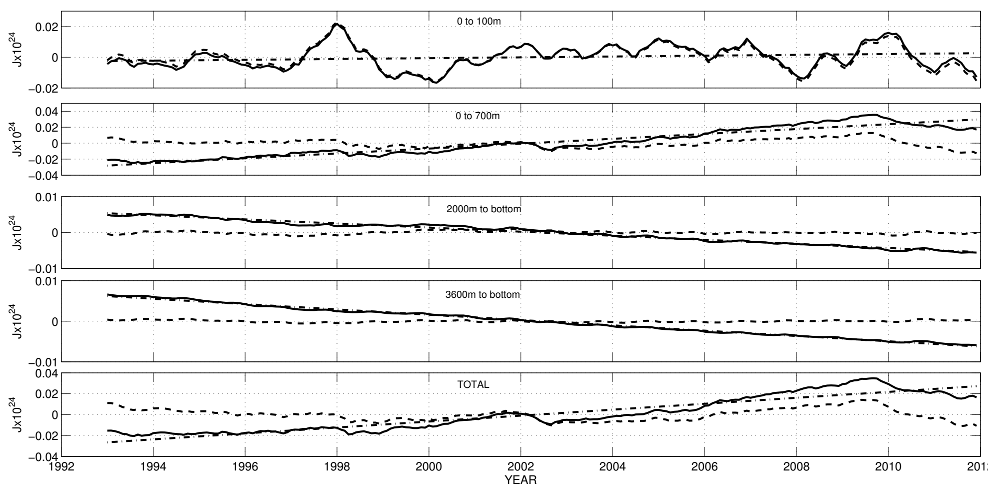

Figure 19: The same as Fig. 18 except the annual cycle has been removed. Dashed-dot lines are the best linear fits, and dashed lines are the residual. The 1997-1998 ENSO event is visible primarily in $I_H\left(0,-100,t\right)$, but can also be detected below where the thermal anomaly is largely compensated. Because of the very long time scales embedded in the oceans, no particular significance is attached here to the apparent linear trends where visible, as they may well be fragments of much longer rednoise trends or systematic errors.

{h_ts_noann.ep

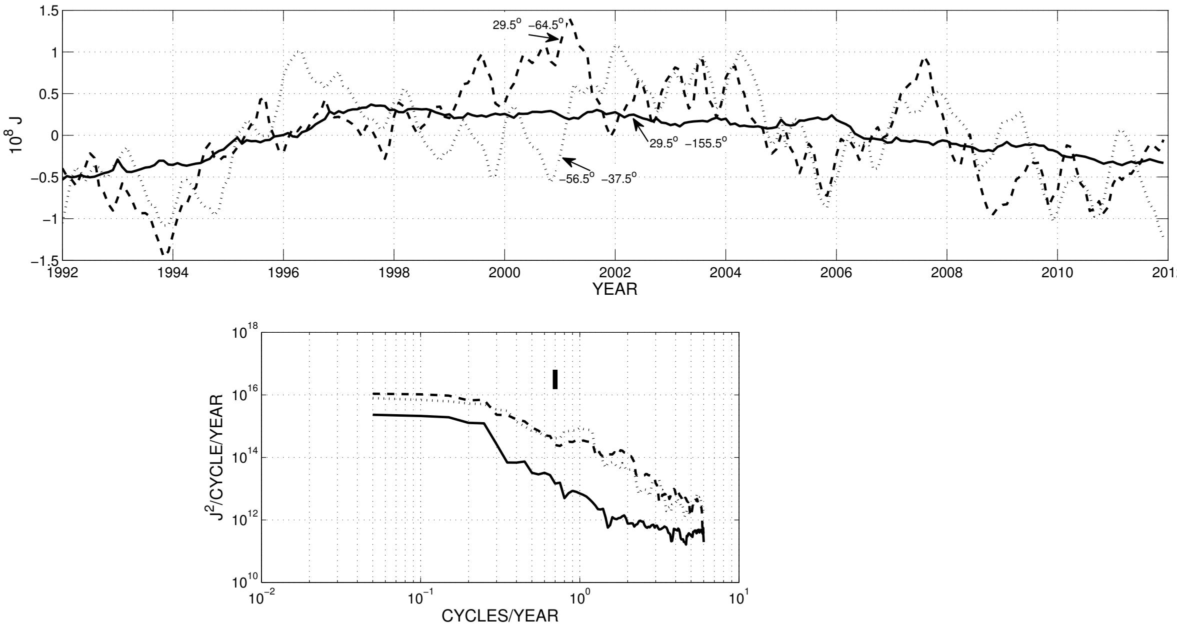

Figure 20: (Upper panel) Time series of $H(-2000,-h,t)$ from the eastern Pacific (latitude 29.5°N, longitude 155.5°W), the western Atlantic (latitude 29.5°N, longitude 64.5°W) and the Southern Ocean (latitude 56.5°S, longitude 37.5°W). Note the visually stronger low frequency variability from the Atlantic. (Lower panel) Power density spectral estimates for the three records shown above. All records approach white noise at low frequencies beyond about 10 years period, with an order of magnitude less variance in the Pacific Ocean. A small power excess near the annual period is visible in the Atlantic values. The power laws at high frequencies, s, lie between about -2.2 to -3, although that characterization is over-simplified. Note that multitaper spectral methods are biassed low at the longest periods. Vertical bar is an approximate 95% confidence interval.

{ts_pd_3pts.ep

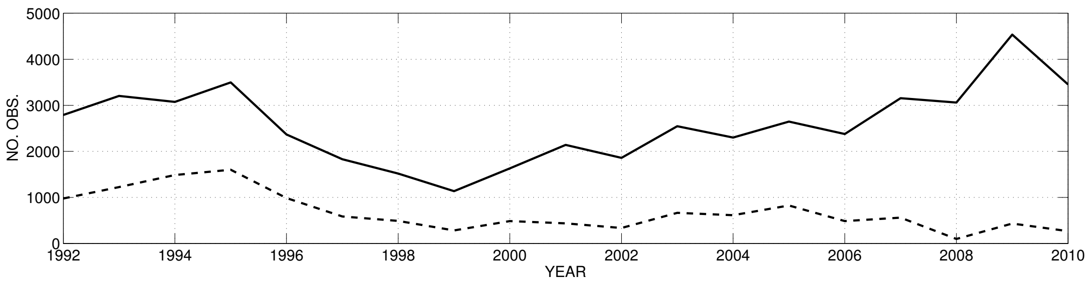

Figure 21: Number of observations extending below 2000 m for each year (solid curve) and below 3600 m (dashed). Upper ocean observations (not shown) greatly increase with the Argo array from the middle 2000s, introducing an important inhomogeneity with time in the estimates.

{nopts_year.ep